

UC Irvine

UC Irvine Previously Published Works

Title

Activated NF- κ B/Nrf2 and Wnt/ β -catenin pathways are associated with lipid metabolism in CKD patients with microalbuminuria and macroalbuminuria

Permalink

<https://escholarship.org/uc/item/148046wd>

Journal

Biochimica et Biophysica Acta (BBA) - Molecular Basis of Disease, 1865(9)

ISSN

0925-4439

Authors

Feng, Ya-Long
Chen, Hua
Chen, Dan-Qian
et al.

Publication Date

2019-09-01

DOI

10.1016/j.bbadis.2019.05.010

Peer reviewed



ELSEVIER

Contents lists available at ScienceDirect

BBA - Molecular Basis of Disease

journal homepage: www.elsevier.com/locate/bbadis

Activated NF- κ B/Nrf2 and Wnt/ β -catenin pathways are associated with lipid metabolism in CKD patients with microalbuminuria and macroalbuminuria

Ya-Long Feng^{a,1}, Hua Chen^{a,1}, Dan-Qian Chen^a, Nosratola D. Vaziri^b, Wei Su^d, Shi-Xing Ma^d, You-Quan Shang^d, Jia-Rong Mao^e, Xiao-Yong Yu^e, Li Zhang^f, Yan Guo^{a,c}, Ying-Yong Zhao^{a,*}

^a School of Pharmacy, Faculty of Life Science & Medicine, Northwest University, No. 229 Taibai North Road, Xi'an, Shaanxi 710069, China

^b Division of Nephrology and Hypertension, School of Medicine, University of California Irvine, 1001 Health Sciences Rd, Irvine, CA 92897, USA

^c Department of Internal Medicine, University of New Mexico, Comprehensive Cancer Center, Albuquerque, NM 87131, USA

^d Department of Nephrology, Baoji Central Hospital, No. 8 Jiangtan Road, Baoji, Shaanxi 721008, China

^e Department of Nephrology, Shaanxi Traditional Chinese Medicine Hospital, No. 2 Xihuamen, Xi'an, Shaanxi 710003, China

^f Department of Nephrology, Xi'an No. 4 Hospital, No. 21 Jiefang Road, Xi'an 710004, China

ARTICLE INFO

Keywords:

Chronic kidney disease
Microalbuminuria
Macroalbuminuria
Inflammation
Lipidomics
Lipid biomarker

ABSTRACT

Early diagnosis of CKD patients at risk for microalbuminuria or macroalbuminuria could facilitate clinical outcomes and long-term survival. Considering the few and limited efficacy of current biomarkers in early detection, we aim to discover plasma lipids that effectively predict the development of CKD patients with microalbuminuria or macroalbuminuria. A total of 380 healthy controls and 1156 patients with CKD stages 3 to 5 were stratified by urine albumin-creatinine ratio as microalbuminuria (30–300 mg/g) and macroalbuminuria (> 300 mg/g). Fasting plasma samples were determined by UPLC-HDMS based on lipidomics. Quantitative real-time polymerase chain reaction, Western blot and immunohistochemical analyses were used to validate the lipid metabolism-associated pathways. Pathway analysis demonstrated that these lipids were closely associated with PPAR γ , inflammatory mediator regulation of TRP channels and RAS signaling, which were intimately involved in activated NF- κ B and Nrf2 pathways. We further carried out pathway validation and demonstrated that NF- κ B pathway was activated in patients with macroalbuminuria compared with CKD patients with microalbuminuria, while Nrf2-associated protein expression was downregulated, which was accompanied by the up-regulation of Wnt/ β -catenin signaling pathway. Four lipids including DTA, 5,8-TDA, GGD3 and DHA that showed great potential in the discrimination of CKD patients with microalbuminuria and healthy controls were selected by logistic regression analysis. Additionally, six lipid species including CDCA, glucosylceramide, GGD2, TTA, DHA and EDA that contributed to the discrimination of CKD patients with microalbuminuria and macroalbuminuria were selected by logistic LASSO regression. Gangliosides were first identified and might be promising therapeutic targets for CKD patients with the different degree of albuminuria. Collectively, this study first demonstrates the

Abbreviations: 12-LO, 12-lipoxygenase; 5,8-TDA, 5,8-tetradecadienoic acid; ACR, albumin-creatinine ratio; AUC, area under curve; BMI, body mass index; BUN, blood urea nitrogen; CDCA, chenodeoxycholic acid; CKD, chronic kidney disease; COX-2, cyclooxygenase-2; DHA, docosahexaenoic acid; DTA, docosatrienoic acid; EDA, eicosadienoic acid; ESRD, end-stage renal disease; FAO, fatty acid oxidation; FSP1, fibroblast-specific protein 1; GCD, glucosylceramide; GCLM, glutamate-cysteine ligase modifier subunit; GFR, glomerular filtration rate; GGD2, ganglioside GD2 (d18:1/18:0); GGD3, ganglioside GD3 (d18:1/26:0); GPX, glutathione peroxidase; HCA, hierarchical cluster analysis; HDL-C, high density lipoprotein-cholesterol; HO-1, heme oxygenase-1; iNOS, inducible nitric oxide synthase; IPA, Ingenuity Pathway Analysis; I κ B α , inhibitor of kappa B alpha; Keap1, Kelch-like ECH-associated protein 1; LASSO, least absolute shrinkage and selection operator; LDL-C, low density lipoprotein-cholesterol; MAPK, mitogen-activated protein kinase; MCP-1, monocyte chemoattractant protein-1; MMP-7, matrix metalloproteinase-7; MRM, multiple-reaction-monitoring; NAD(P)H, nicotinamide adenine dinucleotide phosphate; NF- κ B, nuclear factor-kappa B; NQO1, NAD(P)H quinone oxidoreductase 1; Nrf2, nuclear factor-erythroid-2-related factor 2; OPLS-DA, orthogonal partial least squares-discriminant analysis; PAI-1, plasminogen activator inhibitor-1; PCA, principle component analysis; p-I κ B α , phosphorylated-I κ B α ; PKC, protein kinase C; PLS-DA, partial least-squares discriminant analysis; PPAR γ , peroxisome proliferator-activated receptor γ ; PUFA, polyunsaturated fatty acids; qRT-PCR, quantitative real-time polymerase chain reaction; Rac1, ras-related C3 botulinum toxin substrate 1; ROC, receiver operating characteristic; SFA, saturated fatty acids; TC, total cholesterol; TG, triglycerides; TRP, transient receptor potential; TTA, tetracosatetraenoic acid (24:4n-6); UPLC-HDMS, ultra performance liquid chromatography-high-definition mass spectrometry; VLDL-C, very low density lipoprotein-cholesterol

* Corresponding author.

E-mail address: zyy@nwu.edu.cn (Y.-Y. Zhao).

¹ These authors contributed equally to the study.

<https://doi.org/10.1016/j.bbadis.2019.05.010>

Received 19 March 2019; Received in revised form 10 May 2019; Accepted 13 May 2019

0925-4439/© 2019 Elsevier B.V. All rights reserved.

association of plasma inflammation, oxidative stress, Wnt/ β -catenin and lipid metabolism in CKD patients with microalbuminuria and macroalbuminuria.

1. Introduction

Chronic kidney disease (CKD) is an independent risk factor of cardiovascular diseases [1,2], and CKD patients are more likely to die of cardiovascular diseases rather than enter dialysis. Albuminuria is one of the manifestations in renal diseases. Microalbuminuria (urinary albumin excretion between 30 and 300 mg/day) is regarded as a typical hallmark of kidney dysfunction, which often leads to macroalbuminuria and end-stage renal disease (ESRD) [3]. CKD and heavy glomerular albuminuria (nephrotic syndrome) result in profound but distinctly different changes in plasma lipid metabolism and lipid profile [4]. The dysregulated lipid metabolism are intimately implicated in the progression of CKD and other complications, including accelerated atherosclerosis and cardiovascular diseases, impaired energy metabolism and diminished exercise capacity [5]. The degree of lipid disorders in patients with kidney disease is independently determined by the extent of renal failure and presence and severity of albuminuria [6]. Nephrotic albuminuria resulted in significant elevation of serum total cholesterol (TC), triglycerides (TG), low density lipoprotein-cholesterol (LDL-C), very low density lipoprotein-cholesterol (VLDL-C) and lipoprotein(a), as well as significant changes in the composition of lipoproteins including TC/TG, free cholesterol/cholesterol ester, and phospholipid/lipoprotein ratios [4]. The dysfunction of lipid and lipoprotein in chronic renal failure was primarily caused by the altered expression of proteins involved in production, transport, remodeling, and clearance of lipids and lipoproteins [7,8]. Additionally, nephrotic syndrome led to profound changes in the structure and function of high density lipoprotein-cholesterol (HDL-C) which were caused by the dysregulation of proteins involved in the regulation of HDL-C structure and loading and unloading of its lipid contents [9].

Serum lipid profile in majority of CKD patients without macroalbuminuria and most patients with ESRD on chronic hemodialysis were marked by elevated serum TG, VLDL-C, chylomicron remnants, oxidized lipids and lipoproteins as well as low plasma levels of ApoA1 and HDL-C [4,10]. However, serum TG and LDL-C levels were within or

below the normal limits in most CKD patients without nephrotic proteinuria and ESRD patients on hemodialysis. The LDL-C in this population consisted of small-dense particles containing significant amounts of TG [6]. Finally, due to its impaired clearance, plasma HDL-C level was elevated in a minority of ESRD patients who exhibited a paradoxically higher risk of overall and cardiovascular morbidity and mortality [9].

Inflammation plays a paramount role in the pathogenesis and progression of CKD, which contributes to the albuminuria in CKD [11,12]. Plasma proteomics has demonstrated that CKD patients with hypertension or type 2 diabetes from microalbuminuria to macroalbuminuria stages were closely associated with phosphatidylinositol 3-kinase-Akt-mammalian target of rapamycin, vascular endothelial growth factor and mitogen-activated protein kinase (MAPK) signaling pathways, hinting inflammation is a powerful driver of progressive renal diseases [13]. Additionally, the activation of Wnt signaling pathway was also involved in the development of CKD patients from microalbuminuria to macroalbuminuria [13], which was reactivated in myriad CKD including adriamycin nephropathy, obstructive nephropathy, diabetic nephropathy, chronic allograft nephropathy and polycystic kidney diseases [14].

Although the underlying mechanisms of dysregulated serum lipid and lipoproteins in the progression of CKD and nephrotic syndrome are well-known, their effects on the serum lipid metabolites have not been fully elucidated. A growing body of evidence revealed that sphingomyelin was associated with diabetic kidney disease patients with microalbuminuria or macroalbuminuria and sphingomyelin was recognized as a significant regressor of urinary albumin excretion, which may be exploited for novel biomarker [15]. In the past few years, metabolomics including lipidomics has been increasingly used to detect the dynamic changes of lipid metabolites and identify promising biomarkers of various diseases [16–19]. Moreover, The most compelling evidence indicated that dysregulation of lipid metabolism may contributed to the pathogenesis and progression of CKD [20–24]. Among many analytical platform, ultra performance liquid chromatography-

Table 1

Summary of clinical and demographic baseline characteristics of patients with CKD and healthy controls in this study.

Clinical variables	Healthy controls	CKD patients with microalbuminuria	CKD patients with macroalbuminuria
Male/female	200/180	248/254	308/346
Age (years)	56.8 (51.2–72.5)	60.5 (50.4–71.8)	59.8 (51.4–74.8)
Diabetes (%)	N/A	28.5	29.4
Hypertension (%)	N/A	74.5	78.4
SBP (mm Hg)	117.2 (107.4–124.5)	137.7 (104.4–184.2) **	140.1 (102.5–181.4) **
DBP (mm Hg)	72.8 (61.4–81.4)	79.6 (64.5–95.7) *	79.8 (62.5–94.1) *
Smoker (%)	12.4	13.4	11.5
BMI (kg/m ²)	23.7 (18.1–27.4)	25.1 (20.1–28.4)	24.6 (21.4–27.9)
eGFR (mL/min/1.73m ²)	99.5 (85.5–114.4)	36.4 (20.4–48.5)**	18.6 (11.2–32.8)**##
Creatinine (mg/dL)	0.7 (0.61–0.9)	2.1 (1.1–2.9)**	2.9 (2.7–5.3)**##
BUN (mg/dL)	13.5 (4.9–19.6)	63.2 (35.4–125.6)**	114.5 (69.5–189.7)**##
Uric acid (mg/dL)	5.2 (3.5–9.8)	7.2 (5.7–12.5)**	7.0 (5.6–13.9)**
Triglyceride (mg/dL)	138.0 (87.6–190.3)	148.7 (87.7–209.8)*	165.2 (115.9–224.1)**##
Total cholesterol (mg/dL)	183.6 (139.2–228.2)	197.6 (141.5–253.6)*	219.9 (179.0–274.9)**##
LDL-cholesterol (mg/dL)	93.4 (49.4–137.4)	105.7 (52.5–3.94)*	124.1 (71.8–170.6)**##
HDL-cholesterol (mg/dL)	49.8 (24.7–76.6)	46.1 (27.4–64.6)	39.1 (25.9–52.2)**
Albumin (g/dL)	4.5 (4.0–5.4)	4.2 (4.2–4.8)	4.1 (3.4–5.1)*
Urine ACR (mg/g)	N/A	163.4 (98.9–207.5)	669.5 (511.8–1157.4) ##
White blood cell ($\times 10^9/L$)	5.9 (4.1–8.1)	9.2 (6.77–11.1)**	9.3 (6.3–11.9)**
Hemoglobin (g/dL)	14.2 (13.0–16.6)	11.5 (8.8–13.6)**	9.7 (7.4–11.6)**

Data reported as number (%) or median (interquartile range). * Patients were classified based on albuminuria (urine albumin-creatinine ratio) as microalbuminuria (30–300 mg/g) and macroalbuminuria (> 300 mg/g). * P < 0.05, ** P < 0.01 compared with healthy control group, # P < 0.05, ## P < 0.01 compared with CKD patients with microalbuminuria. BMI, body mass index; eGFR, estimated glomerular filtration rate (4-variable Modification of Diet in Renal Disease formula); ACR, albumin-creatinine ratio; SBP, systolic blood pressure; DBP, diastolic blood pressure. N/A, not available.

Table 2

Clinical variable associations of healthy controls vs CKD patients from logistic regression analysis and linear regression analysis of clinical variables vs ACR.

Clinical variables	Healthy controls vs microalbuminuria			Clinical variables vs ACR		
	Effect	StdErr	p	Effect	StdErr	p
Sex	-0.2166	0.1364	1.12E-01	27.0885	18.8324	1.51E-01
Age	0.0019	0.0040	6.40E-01	1.5074	0.5846	1.00E-02
SBP	0.0423	0.0040	5.30E-26	0.8916	0.2749	1.22E-03
DBP	0.0344	0.0053	8.78E-11	2.5061	0.6049	3.68E-05
BMI	0.0855	0.0198	1.50E-05	3.1176	2.5770	2.27E-01
BUN	1.0095	0.3105	1.15E-03	4.8222	0.1455	1.02E-169
Creatinine	25.4823	4.4394	9.46E-09	-	-	-
Uric acid	0.5896	0.0492	4.90E-33	9.0564	4.2966	3.53E-02
TG	0.0008	0.0009	3.66E-01	-0.0113	0.0796	8.87E-01
TC	0.0019	0.0008	1.46E-02	0.5774	0.1411	4.60E-05
HDL-C	-0.0045	0.0038	2.36E-01	-3.4485	0.6710	3.24E-07
LDL-C	0.0072	0.0017	2.17E-05	1.0406	0.1661	5.24E-10
White blood cell	0.4232	0.0372	5.04E-30	3.0302	2.3915	2.05E-01
Hemoglobin	-0.2326	0.0226	7.82E-25	-18.6774	2.7078	8.70E-12

high-definition mass spectrometry (UPLC-HDMS) has been increasingly applied to lipidomics or lipid identification [25–31]. Given the profound impact of microalbuminuria or macroalbuminuria on lipid metabolism, we conducted a population-based cohort study to examine gene and protein expression on a group of stage 3 to 5 CKD patients with microalbuminuria and macroalbuminuria by using UPLC-HDMS. The aim of the current study is to discover specific lipid species that could stratify CKD patients between microalbuminuria and macroalbuminuria and provide potential additional biomarkers to predict the progression of renal dysfunction. Additionally, identified metabolic pathways that played pivotal roles in aberrant lipid metabolism were further validated by molecular biology approach.

2. Materials and methods

2.1. Study population

A prospective, case-control study was performed in multiple medical centers in China from January 2013 to December 2017 from the Shaanxi Traditional Chinese Medicine Hospital, Xi'an No. 4 Hospital and Baoji Central Hospital. CKD patients aged > 18 years old are eligible for the current study. CKD was defined by the criteria of either kidney injury or declining glomerular filtration rate (GFR) for at least three months [32]. The urine albumin-creatinine ratio was measured by dividing the urine albumin to creatinine concentration. Proteinuria based on albumin-creatinine ratio was defined as normoalbuminuria (< 30 mg/g), microalbuminuria (30–300 mg/g) and macroalbuminuria (> 300 mg/g). Patients with current infection, malignancy, pregnancy, kidney transplant and dialysis are excluded. All patients are maintained on their regular medication. 380 age-matched healthy controls with no history of kidney disease were enrolled. The study was conducted in accordance with the Helsinki declaration and approved by the ethics committees of the above institutions. Signed informed consents were obtained from all patients prior to their inclusion in the study.

2.2. Hypertension, diabetes and dyslipidemia definition

CKD patients were stratified as the use of anti-hypertensive treatment (self-reported or information retrieved from the regional pharmacy database) or systolic/diastolic blood pressure \geq 140/90 mm Hg. Diabetes was stratified by historical blood glucose concentrations based on the criteria of American Diabetes Association, oral hypoglycemic drug or insulin use. Dyslipidemia was defined as fasting triglyceride \geq 200 mg/dL, total cholesterol \geq 200 mg/dL, low-density lipoprotein \geq 130 mg/dL.

2.3. Participants with drug intervention for potential biomarker validation

Based on the analysis of 24-hour proteinuria, an additional 104 patients with CKD were further studied for biomarker validation. 54 and 50 patients with proteinuria between 0.5 and 1.0 g/24h were treated by enalapril (10 mg/kg/d) and Wulingsan (0.15 g/kg/d, a natural renoprotective medicine) in six months, respectively. 32, 37 and 35 patients were diagnosed as immunoglobulin A nephropathy, idiopathic membranous nephropathy and hypertension nephropathy, respectively. A total of 208 serum samples were collected from CKD patients before and after drug treatments.

2.4. Untargeted lipidomics

Lipid profiling procedure of UPLC-HDMS was performed by the previously published protocols [10]. Lipidomics was performed on a Waters Acquity™ ultra performance LC system equipped with a Waters Xevo™ G2-S QToF MS. Each sample was injected onto a reverse-phase 100 \times 2.1 mm, HSS 1.7 μ m C₁₈ column using an ACQUITY UPLC system (Waters Corporation, USA). A gradient of 10 mM ammonium formate and 0.1% formic acid in 2-propanol/acetonitrile (90/10) (A) and 10 mM ammonium formate and 0.1% formic acid in ACN/H₂O (60/40) (B) were used as follows: a linear gradient of 0–10 min, 40.0–99.0% A and 10.0–12.0 min, 99.0–40.0% A. The flow rate was 0.5 mL/min. The temperatures of autosampler and chromatographic column were maintained at 4 °C and 55 °C, respectively. Every 5 μ L sample solution was injected for each run.

Mass spectrometry was performed on a Xevo™ G2 QToF. The scan range was from 100 to 1500 *m/z*. For both positive and negative electrospray modes, the capillary and cone voltage were set at 3.0 kV and 60 V, respectively. The desolvation gas was set to 900 L/h at a temperature of 500 °C; the cone gas was set to 50 L/h and the source temperature was set at 120 °C. An MS^E experiment was performed as follows: function 1, 10 V collision energy; function 2, collision energy ramp of 20–65 V. Data were collected in continuum mode, the lock-spray frequency was set at 10 s, and data were averaged over 10 scans. All the acquisition and analysis of data were controlled by Waters Unifi software.

2.5. Targeted lipidomics

Targeted lipidomics was performed on the same UPLC-HDMS system. Targeted data detection was performed in the multiple-reaction-monitoring (MRM). The reference standard chenodeoxycholic acid (CDCA) was used for the quantification of CDCA. The reference standard docosahexaenoic acid (DHA) was used for the quantification of glucosylceramide (GCD), ganglioside GD2 (d18:1/18:0) (GGD2),

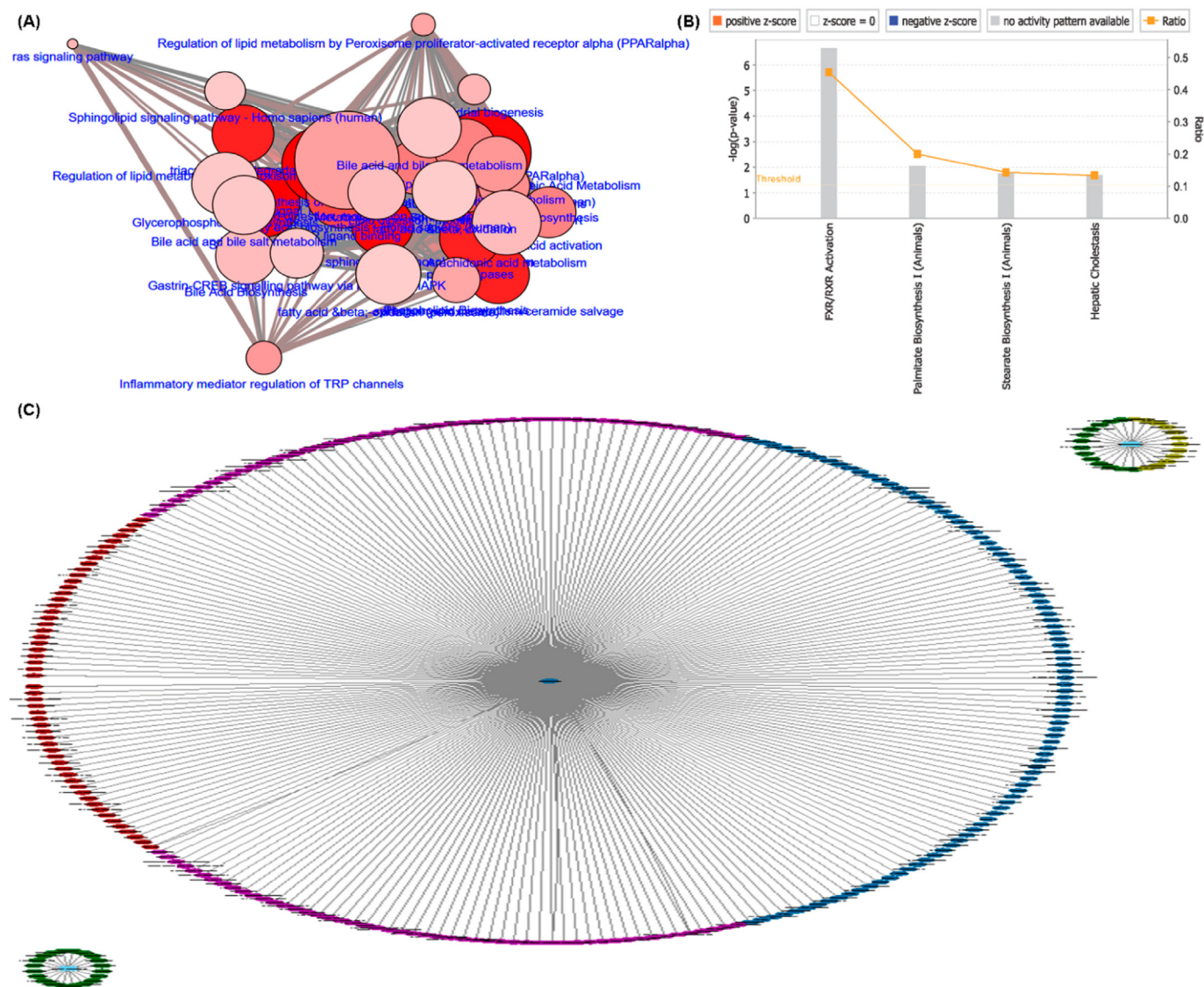


Fig. 1. The association between inflammation and metabolic pathways of identified lipid species in CKD patients with microalbuminuria. (A) The results of pathway enrichment analysis by using the 237 lipid species. The correlation of the genes, proteins and lipid species were identified by the pathways databases. (B) The top affected pathways observed in logistic regression. The significant canonical pathways were displayed along the x-axis, while the y-axis displayed the $-\log$ of p -value which was calculated by right tailed Fisher's exact test. Thus, taller bars represented the increased significance and the canonical pathways were sorted by significance from left to right. White bars were those with a z-score at or very close to 0, while gray bars indicated the pathways that can not be made at present. In addition, the orange points connected by a thin line represented the Ratio. (C) Co-abundance network constructed within Pearson's correlation using the four biomarkers and 303 identified lipid species.

tetracosatetraenoic acid (24:4n-6) (TTA), DHA and eicosadienoic acid (EDA).

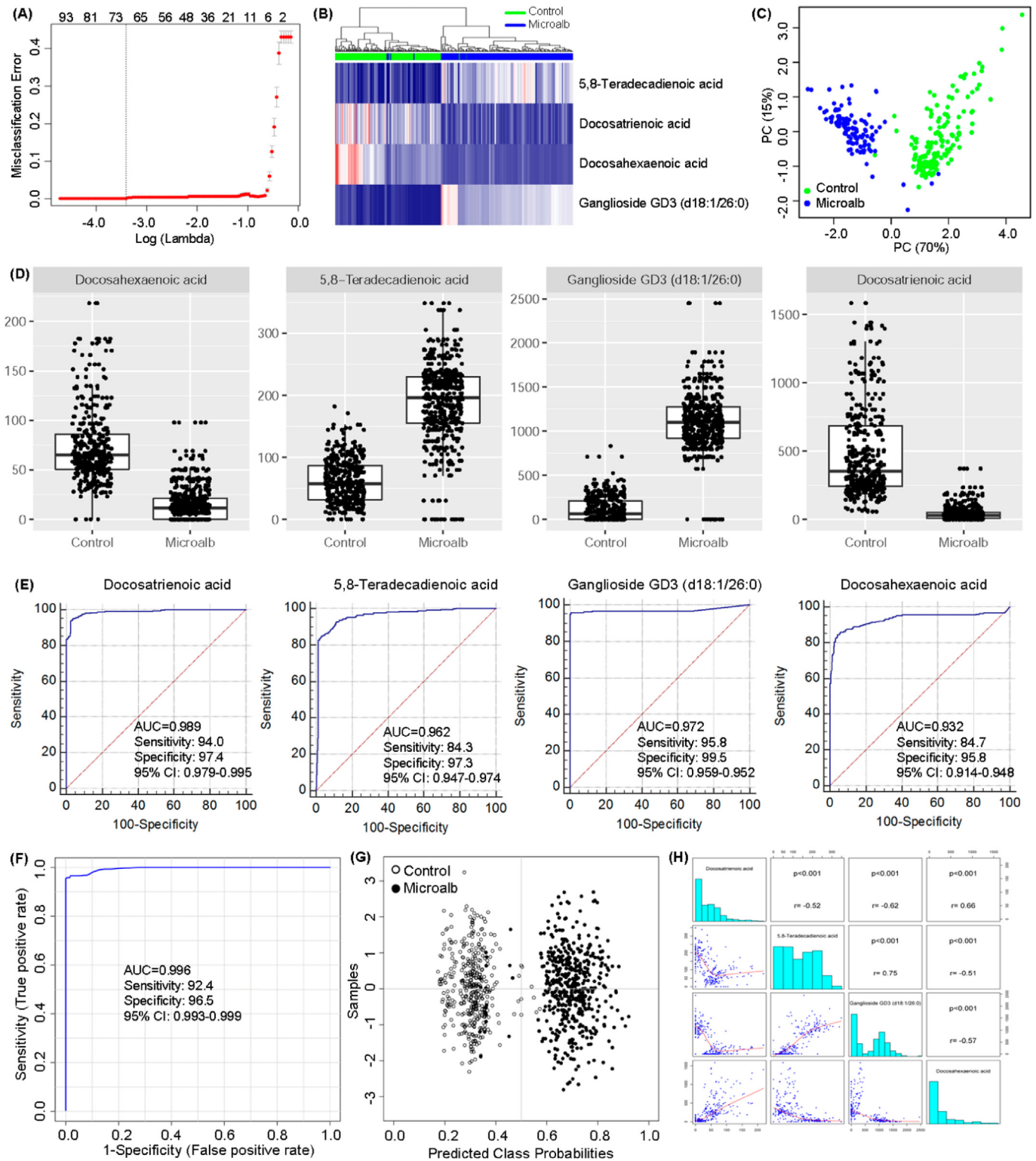
2.6. Lipidomic data analysis

Lipidomics data were collected by mass spectrometry on 1536 participants (healthy controls = 380, CKD patients with microalbuminuria = 502, CKD patients with macroalbuminuria = 654). Mass spectrometry data were normalized to total signal per subject then \log_2 transformed. We used regularization algorithm least absolute shrinkage and selection operator (LASSO) with 10 fold cross validation (GLMNET R package) to identify biomarkers that played prominent roles in the identification of CKD patients with microalbuminuria and healthy controls. Unsupervised machine learning techniques including hierarchical cluster analysis (HCA) and principle component analysis (PCA) were used to validate the accuracy of the biomarkers or lipid metabolites. Univariate logistic regressions were also performed on all

potential lipids to identify all lipids associated with the binary outcome (healthy controls vs CKD patients with microalbuminuria). Additionally, we conducted univariate linear regression by using albumin-creatinine ratio (ACR) of all CKD patients as continuous outcome and lipids as predictors. Furthermore, metabolic pathway analysis was performed by Ingenuity Pathway Analysis (IPA).

2.7. Gene expression studies by quantitative real-time polymerase chain reaction (qRT-PCR)

Isolation of plasma mRNA was performed by a High Pure RNA Isolation Kit according to the manufacturer's guide. qRT-PCR was carried out according to previously published protocols with minor modifications [33].



(caption on next page)

2.8. Protein expression studies by Western blotting analysis and immunohistochemistry

All the antibodies were purchased from Abcam Company, Cell Signaling Technology, R&D Technology or Santa Cruz Biotechnology. The total protein concentration in plasma was determined by Assay Kit. A detailed description of these studies had been reported in previous studies [34,35]. The densitometry of each protein ratio was quantified

by using ImageJ software. The following antibodies including Wnt1, β -catenin, active β -catenin, Twist, Snail1, plasminogen activator inhibitor-1 (PAI-1), matrix metalloproteinase-7 (MMP-7) and fibroblast-specific protein 1 (FSP1) were used for immunohistochemistry from renal biopsies of CKD patients [36–38]. Image analysis was done by Image-Pro Plus 6.0.

Fig. 2. Potential biomarkers of identification, analysis and validation from CKD patients with microalbumin and healthy controls. (A) GLMNET LASSO regression with binary outcome. The plot indicated that the error rate (y-axis) was decreased when the number of predictors (x-axis) was increased, while the diminishing return can be clearly observed. The error rate was < 5% when the number of predictors was eight, and four of the eight predictors were identified as biomarkers including docosatrienoic acid, 5,8-tetradecadienoic acid, ganglioside GD3 (d18:1/26:0) and docosahexaenoic acid. (B) Unsupervised cluster on CKD patients with microalbuminuria and healthy controls (C) Scatter plot of PC1 vs PC2 from PCA. The PC1 can explain 70% of the outcome. (D) Combined box-and-whisker and dot plot of normalized intensity of four biomarkers in the serum of CKD patients with microalbuminuria and healthy controls. The statistical significance of differences between the two groups was marked. $^{***}P < 0.01$ compared with the healthy controls. (E) PLS-DA based ROC curves for the evaluation of CKD patients with microalbuminuria with the individual lipid biomarkers. The associated AUC, sensitivity, specificity and 95% confidence interval (95% CI) values were indicated. (F) PLS-DA based ROC curves of the combination of four biomarkers for evaluation of CKD patients with microalbuminuria. The associated AUC, sensitivity, specificity and 95% confidence interval (95% CI) values were indicated. (G) Diagnostic performance of the four biomarkers based on the PLS-DA model. Black dots represented CKD patients with microalbuminuria, and black circles represented healthy controls. The five black dots located healthy controls quadrant and 20 black circles located patients with microalbuminuria were for the incorrectly predicted samples in patients with microalbuminuria and healthy controls, respectively. (B) Correlation matrix of the four biomarkers from CKD patients with microalbuminuria and healthy controls.

Table 3

Logistic regression results for the 4 selected biomarkers.

Lipid	Effect	StdErr	OR(95%CI)	P
Docosatrienoic acid	-9.8E-02	6.4E-03	0.91(0.90-0.92)	1.99E-53
5,8-Tetradecadienoic acid	3.7E-02	2.4E-03	1.04(1.03-1.04)	9.49E-55
Ganglioside GD3 (d18:1/26:0)	8.5E-03	6.0E-04	1.01(1.01-1.01)	9.79E-46
Docosahexaenoic acid	-2.9E-02	2.1E-03	0.97(0.97-0.98)	6.78E-43

3. Results

3.1. Clinical characteristics

Total 1156 patients with CKD stage 3 to 5 were analyzed (Table 1), which were divided into two groups according to the urine ACR. Of all patients, 43.5% ($n = 502$) and 56.5% ($n = 654$) CKD patients had microalbuminuria and macroalbuminuria, respectively. There was significant elevation of serum creatinine, blood urea nitrogen (BUN), TG, TC and LDL-C in CKD patients. Additionally, anemia was more severe in both microalbuminuria and macroalbuminuria groups than healthy controls. Compared with CKD patients with microalbuminuria, patients with macroalbuminuria had a significant increase in serum creatinine, BUN, TG, TC and LDL-C. Decreased HDL-C and albumin were evident in patients with macroalbuminuria. Comparison of data between CKD subgroups revealed CKD patient with macroalbuminuria exhibited significantly lower HDL-C and albumin levels in relative to CKD patient with microalbuminuria.

14 clinical variables were analyzed by univariate logistic regression (Table 2). Systolic blood pressure (SBP), diastolic blood pressure, body mass index (BMI), BUN, creatinine, uric acid, TC, LDL-C and white blood cell were positively associated with CKD patients with microalbuminuria, while hemoglobin was negatively significantly associated with CKD patients with microalbuminuria. Furthermore, univariate linear regression was also used to evaluate the association of these 14 clinical variables with ACR among CKD patients (Table 2), and showed that SBP, BUN, uric acid, TC and LDL-C were positively associated with ACR.

3.2. Correlation analysis of genes, proteins and lipids in CKD patients with microalbuminuria

We obtained 4776 and 2773 spectral features in positive and negative ion modes. After rigorous quality control and multiple test adjustment, 2098 features were chosen by using logistic regression analysis between controls and CKD patients with microalbuminuria. After excluding xenobiotics and different fragment ions from the same lipids, 293 lipids were identified using logistic regression analysis between controls and CKD patients (Supplementary Table S1). These results imply that there is large difference in lipid abundance between healthy controls and CKD patients. Pathway enrichment analysis of 293 lipids

showed that 31 metabolic pathways were associated with CKD patients (Fig. 1A), among which some metabolic pathways played prominent roles in the regulation of lipid metabolism including peroxisome proliferator-activated receptor γ (PPAR γ), inflammatory mediator regulation of transient receptor potential (TRP) channels, RAS signaling pathway, α -linolenic acid and linoleic acid metabolism, fatty acid β -oxidation, unsaturated fatty acid biosynthesis, sphingolipid metabolism, arachidonic acid metabolism, bile acid biosynthesis and gastrin-CREB signaling pathway via protein kinase C (PKC) and MAPK. PPAR γ was of paramount importance to lipid metabolism, and TRP channels contributed much to inflammatory mediator regulation, while RAS signaling pathway were implicated in inflammation and oxidative stress, all of which are inseparably involved in the activation of nuclear factor-kappa B (NF- κ B) and nuclear factor-erythroid-2-related factor 2 (Nrf2) signaling pathways in the current study. Additionally, we used identified lipids from each analysis to examine what pathway they affect by IPA, and discovered that the top affected pathways observed in logistic regression were intimately associated with farnesoid X receptor (FXR)/retinoid X receptor (RXR) activation, palmitate biosynthesis, stearate biosynthesis and hepatic cholestasis (Fig. 1B). These findings indicate that identified lipids are primarily associated with fatty acid and bile acid metabolisms. Moreover, IPA analysis showed that FXR/RXR activation was one of most important pathways in CKD patients. FXR is mainly expressed in the liver, intestine and kidney. Bile acids participate in the regulation of gene expression through acting as ligands for the FXR [39], indicating FXR may be an attractive target for liver and kidney disease intervention. Halilbasic *et al.* uncovered that FXR agonists were used for the treatment of liver disease [40], providing additionally evidence to previous studies. Taken together, these findings indicate that identified lipids, especially for fatty acids, are closely associated with the activation of FXR/RXR and NF- κ B/Nrf2 signaling pathways.

3.3. Biomarkers of identification and validation in CKD patients with microalbuminuria

To select the promising lipids that can be used as biomarkers to detect CKD patients, we conducted feature selection analysis by using logistic regression with 10 fold cross validation with LASSO procedure (R GLMNET). The model with the lowest misclassification error rate (< 1%) can be achieved with 93 features (Fig. 2A) and 66 lipids can be identified from these 93 features (Supplementary Table S1). The same model also revealed that an error rate < 5% can still be achieved by selecting four most relevant lipids. We identified these four biomarkers including docosatrienoic acid (DTA), 5,8-tetradecadienoic acid (5,8-TDA), ganglioside GD3 (d18:1/26:0) (GGD3) and DHA (Fig. 2A). The distribution and pairwise relationship of these four lipids were illustrated with Fig. 2B.

To highlight the co-abundance network of the four potential biomarkers and other metabolites, 925 variables were chosen based on Pearson's correlation and 303 lipids were identified (Table S2). A co-abundance network between the four biomarkers and 303 lipids was

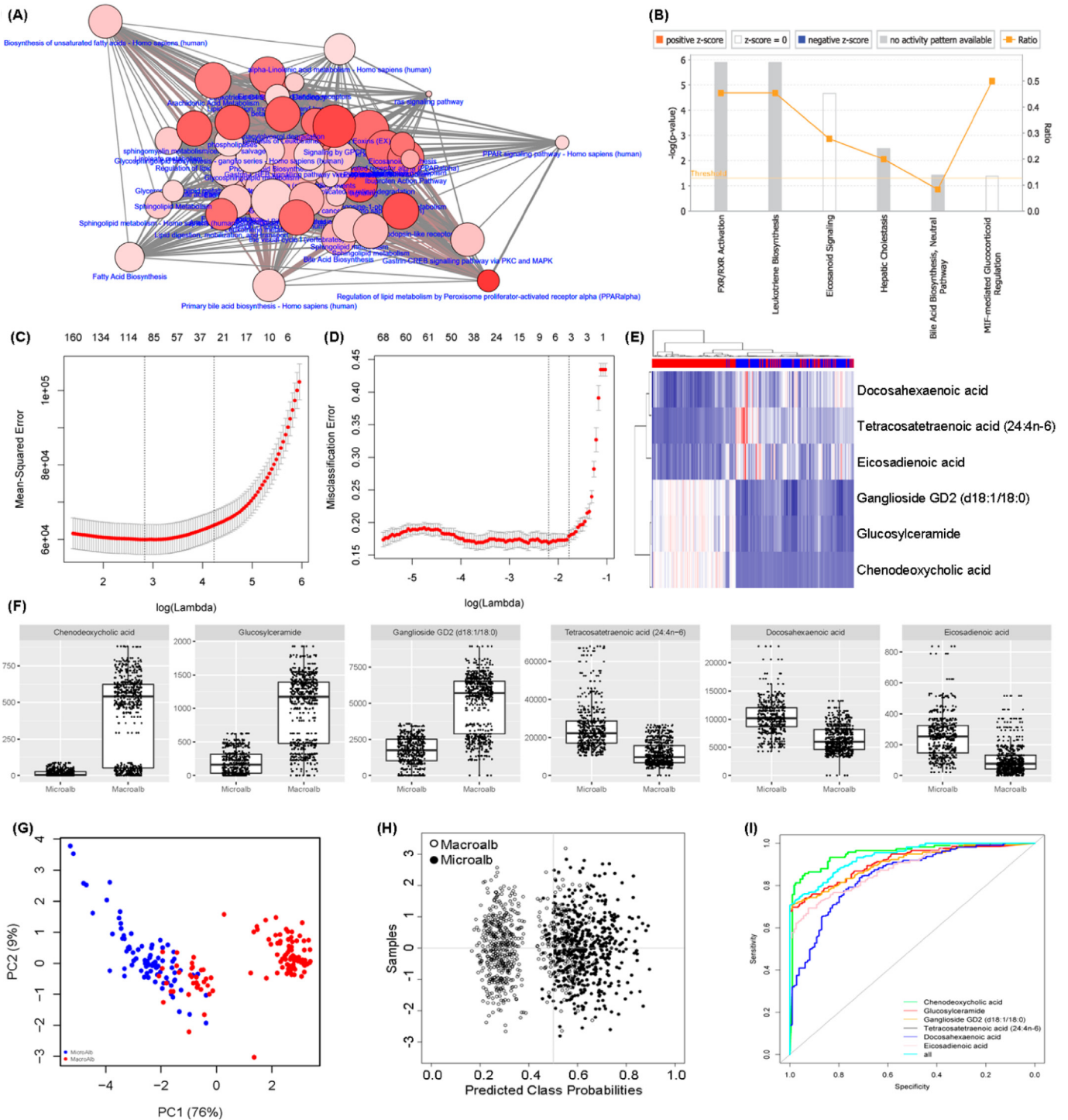


Fig. 3. Biomarker identification and pathway analysis. (A) The results of pathway enrichment analysis of 237 lipid species. The correlation of the genes, proteins and lipid species were identified by the pathways databases. (B) The results of canonical pathway analysis from IPA. The ACR equalled to the results of 237 identified lipid species analysis from linear regression. (C) GLMNET LASSO regression with linear outcome. Y-axis represented mean-square error, and the results were the lower the better. X-axis represented the number of predictors. In general, the mean-square error was reduced with the increased number of predictors. (D) GLMNET LASSO regression with binary outcome. The plot indicated that the error rate (y-axis) was decreased when the number of predictors (x-axis) was increased. (E) Unsupervised cluster on CKD patients with microalbuminuria and macroalbuminuria. (F) Combined box-and-whisker and dot plot of normalized intensity of four biomarkers in the serum of CKD patients with microalbuminuria and healthy controls. (G) Scatter plot of PC1 vs PC2 from PCA. The two groups were evidently separated based on the six biomarkers, and the PC1 can explain 76% of the outcome. (H) Diagnostic performance of the six biomarkers based on the PLS-DA model. Black dots represented CKD patients with microalbuminuria, and black circles represented CKD patients with macroalbuminuria. The 20 black dots located patients with macroalbuminuria quadrant and 175 black circles located patients with microalbuminuria quadrant were for the incorrectly predicted samples in patients with microalbuminuria and macroalbuminuria, respectively. (I) PLS-DA based ROC curves of six biomarkers for the evaluation of the individual lipid biomarkers and the combination of six lipid biomarkers in CKD patients with microalbuminuria.

Table 4
Logistic regression results for the 6 selected biomarkers.

Lipid	Effect	StdErr	OR(95%CI)	P
Chenodeoxycholic acid	2.6E-02	3.6E-03	1.03(1.02-1.03)	1.41E-13
Glucosylceramide	5.5E-03	3.8E-04	1.01(1.00-1.01)	3.00E-49
Ganglioside GD2 (d18:1/18:0)	1.2E-03	7.9E-05	1.00(1.00-1.00)	2.31E-55
Tetracosatetraenoic acid (24:4n-6)	-2.3E-04	1.3E-05	1.00(1.00-1.00)	7.85E-65
Docosahexaenoic acid	-5.6E-04	3.3E-05	1.00(1.00-1.00)	7.16E-64
Eicosadienoic acid	-1.2E-02	7.3E-04	0.99(0.99-0.99)	2.21E-57

obtained from Pearson's correlation coefficients by using MetScape software running on Cytoscape (Fig. 1C). The co-abundance network indicated that there was a strong interaction in four biomarkers, especially for DTA and 303 lipids.

Validation of these four lipid biomarkers was carried out by using two unsupervised machine learning techniques: HCA (Fig. 2B) and PCA (Fig. 2C). The abundance of four biomarkers between CKD patients and controls can be visualized in Fig. 2D. The odds ratio and 95%CI for the four biomarkers from logistic regression can be seen in Table 3. In order to investigate the biomarker suitability, partial least-squares discriminant analysis (PLS-DA)-based receiver operating characteristic (ROC) curves for the evaluation of CKD patients with the individual lipids and the combination of the four lipids were assessed. The combination of the four lipids had a higher area under curve (AUC), sensitivity and specificity than that of individual lipids (Fig. 2E,F). To predict class probabilities for each sample, validation was performed on four biomarkers (Fig. 2G). 482 out of the 502 CKD patients with microalbuminuria were correctly grouped (96.0% sensitivity). 375 out of the 380 healthy controls were located in the control area (98.6% specificity). These results demonstrate that the four biomarkers show high prediction class probabilities. Both methods yield highly accurate results and demonstrate that CKD patients can be distinguished from controls (Fig. 2H).

3.4. Correlation of genes, proteins and lipids in CKD patients with macroalbuminuria

Rather than treating ACR as a discreet dichotomized variable (microalbuminuria vs macroalbuminuria), ACR was recognized as a continuous variable because the division between CKD patients with microalbuminuria vs macroalbuminuria was arbitrary. The regression model identified 2389 features with significant association with ACR. We selected the top 500 significant features and 245 lipids were identified (Table S3). Pathway enrichment analysis of these 245 lipids showed that 54 metabolic pathways were associated with macroalbuminuria changes in CKD patients (Fig. 3A). Identified lipid-associated with metabolic pathways were primarily focused on the regulation of lipid metabolism by PPAR γ , RAS signaling pathway, α -linolenic acid metabolism, unsaturated fatty acids biosynthesis, fatty acid β -oxidation, arachidonic acid metabolism as well as primary bile acid biosynthesis and gastrin-CREB signaling pathway via PKC and MAPK (Fig. 3A). These metabolic pathways, especially for PPAR γ and RAS signaling pathways, were closely associated with inflammation and oxidative stress, which are consistent with the activation of NF- κ B/Nrf2 signaling pathway in the current study. Additionally, we used the identified lipids from each analysis to examine what pathway they affect. IPA demonstrated that the top affected pathway for results from linear regression was associated with FXR/RXR activation (Fig. 3B).

3.5. Lipid identification from CKD patients with ACR association

Apart from above-mentioned factors, we also conducted feature selection by linear regression with 10 fold cross validation with LASSO

procedure. The model found the least mean square error can be achieved when 98 features were used (Fig. 3C), and 66 lipid species were identified from these 98 features (Table S4). Furthermore, we also conducted biomarker analysis by logistic LASSO regression with 10 fold cross validation to dichotomize patients into two groups of microalbuminuria and macroalbuminuria (Fig. 3D). Six lipids including CDCA, GCD, GGD2, TTA, DHA and EDA were identified by the model. The odds ratio and 95%CI for six biomarkers from logistic regression can be seen in Table 4. The validation of HCA (Fig. 3E) and PCA (Fig. 3G) also showed reasonable separation between CKD patients with microalbuminuria and macroalbuminuria. The abundance of six biomarkers between CKD patients with microalbuminuria and macroalbuminuria can be visualized in Fig. 3F. Sensitivity and specificity of six biomarkers were 96.0% and 73.2%, respectively (Fig. 3H). In addition, ROC curves showed that the combination of the six lipids had a lower AUC, sensitivity and specificity than that of CDCA (Fig. 3I).

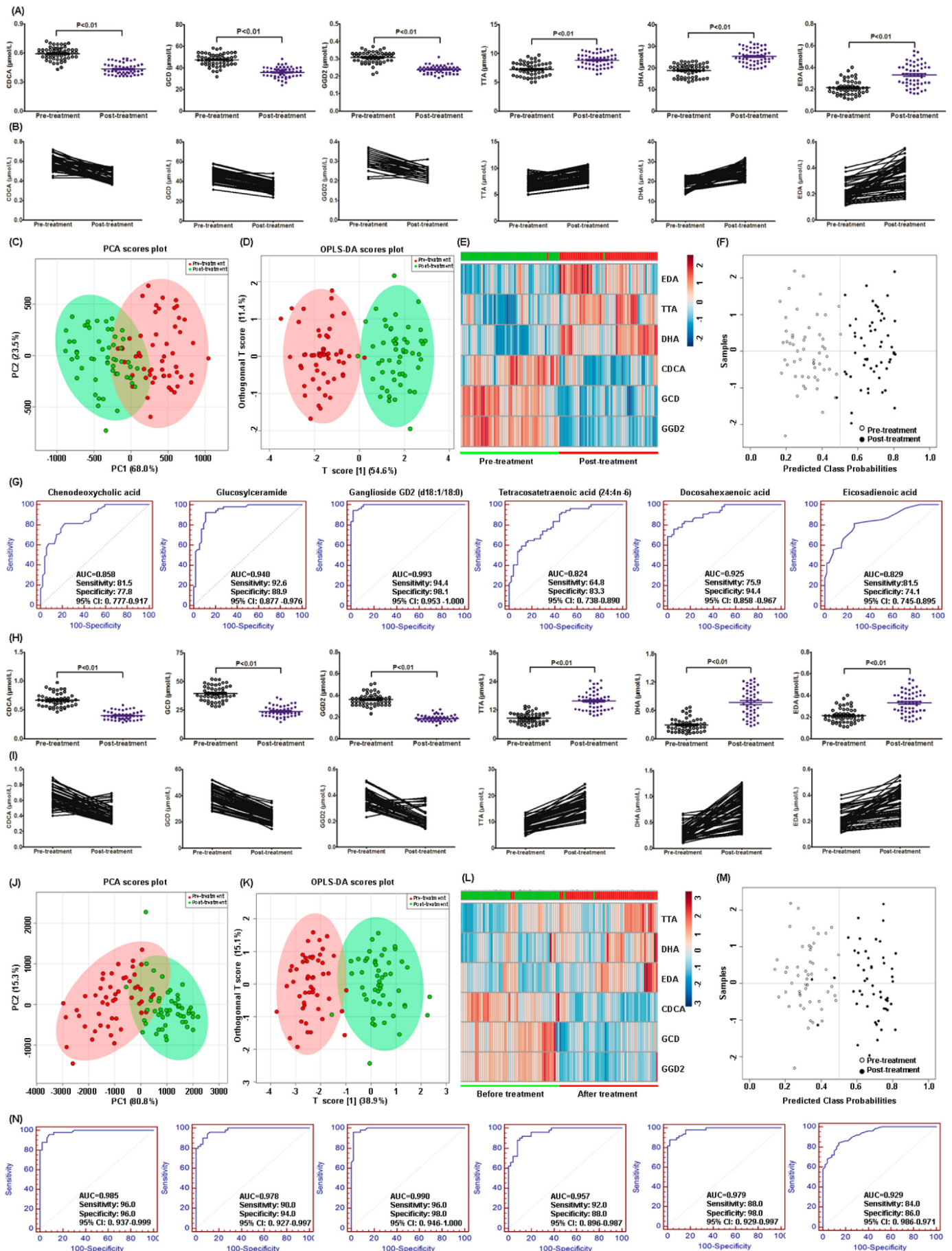
3.6. Biomarker validation of CKD patients with macroalbuminuria after drug treatment

Next we examined whether enalapril and Wulingsan could improve abnormal biomarkers that were applied to drug use and therapy evaluation (Fig. 4). The significantly increased proteinuria and ACR as well as decreased eGFR in CKD patients were improved after the treatment of enalapril and Wulingsan (Table 5). Moreover, six biomarkers were restored after enalapril treatment (Fig. 4A,B). PCA, orthogonal partial least squares-discriminant analysis (OPLS-DA) and heatmap showed that CKD patients before and after enalapril treatment could be separated by six biomarkers (Fig. 4C-E). Prediction class probabilities showed that the sensitivity and specificity of six biomarkers were 98.1% (Fig. 4F). ROC curves showed that six biomarkers had a high AUC, sensitivity and specificity after enalapril treatment (Fig. 4G). Similarly, six biomarkers were restored after Wulingsan treatment (Fig. 4H,I), and six biomarkers could specially discriminate CKD patients before and after Wulingsan treatment (Fig. 4J-N).

3.7. Gene and protein expression of NF- κ B pathway

In order to further validate the identified lipid-associated inflammatory metabolic pathways, qRT-PCR, Western blot and immunohistochemical analyses were used. Primers applied for qRT-PCR were listed in Supplementary Table S5. Compared with CKD patients with microalbuminuria, CKD patients with macroalbuminuria exhibited a significant up-regulation of I κ B α and nuclear translocation of p65 mRNA expression, indicating activation of NF- κ B signaling (Fig. 5A). In addition, the activation of I κ B/NF- κ B signaling was accompanied by up-regulation of inflammatory genes including cyclooxygenase-2 (COX-2), inducible nitric oxide synthase (iNOS), monocyte chemoattractant protein-1 (MCP-1) and 12-lipoxygenase (12-LO) as well as NAD(P)H oxidase subunit genes such as p47^{phox} and gp91^{phox}, while p67^{phox} mRNA expression was not significantly altered in CKD patients with macroalbuminuria.

Compared with CKD patients with microalbuminuria, the protein expression of the inhibitor of kappa B alpha (I κ B α) was significantly decreased, while the expression of phosphorylated-I κ B α (p-I κ B α) and nuclear p65 contents denoting NF- κ B activation was significantly increased in the plasma of CKD patients with macroalbuminuria (Fig. 5B). Additionally, the ratio of p-I κ B α /I κ B α was also significantly increased in CKD patients with macroalbuminuria, which was accompanied by a significant increase in protein abundance of the nicotinamide adenine dinucleotide phosphate (NAD(P)H) oxidase subunits including ras-related C3 botulinum toxin substrate 1 (Rac1), p67^{phox}, p47^{phox} and gp91^{phox} and up-regulation of COX-2, iNOS, MCP-1 and 12-LO in CKD patients (Fig. 5B).



(caption on next page)

Fig. 4. Biomarker validation of CKD patients with macroalbuminuria after drug treatment. (A) Dot plots of levels of six biomarkers including CDCA, GCD, GGD2, TTA, DHA and EDA in CKD patients before and after enalapril treatment, which were determined by UPLC-MS/MS method. (B) Arrow plot of changes of six biomarkers from CKD patients before and after enalapril treatment. (C) PCA of two components of six biomarkers from 54 CKD patients before and after enalapril treatment. (D) OPLS-DA of six biomarkers from 54 CKD patients before and after enalapril treatment. (E) Heatmap of six biomarkers from 54 CKD patients before and after enalapril treatment. (F) Diagnostic performances of the six biomarkers from CKD patients before and after enalapril treatment based on the PLS-DA model. The one black dot located pre-treatment patient's quadrant and one black circle located post-treatment patient's quadrant were for the incorrectly predicted samples in patients before and after treatment, respectively. (G) PLS-DA based ROC curves of six biomarkers for evaluation of CKD patients before and after enalapril treatment. (H) Dot plots of levels of six biomarkers including CDCA, GCD, GGD2, TTA, DHA and EDA in CKD patients before and after Wulinsan treatment, which were determined by UPLC-MS/MS method. (I) Arrow plot showing changes of six biomarkers from CKD patients before and after Wulinsan treatment. (J) PCA of two components of six biomarkers from 54 CKD patients before and after Wulinsan treatment. (K) OPLS-DA of six biomarkers from 54 CKD patients before and after Wulinsan treatment. (L) Heatmap of six biomarkers from 54 CKD patients before and after Wulinsan treatment. (M) Diagnostic performances of the six biomarkers from CKD patients before and after Wulinsan treatment based on the PLS-DA model. The three black dot located pre-treatment patient's quadrant and one black circle located post-treatment patient's quadrant were for the incorrectly predicted samples in patients before and after treatment, respectively. (N) PLS-DA based ROC curves of six biomarkers for evaluation of CKD patients before and after Wulinsan treatment. The associated AUC, sensitivity, specificity and 95% confidence interval (95% CI) values were indicated. $**P < 0.01$, compared with CKD patients before treatment.

Table 5

Clinical data and biochemical results of patients before and after treatment with enalapril and Oryeongsan.

Clinical characteristics	Pre-treatment by enalapril	Post-treatment by enalapril	Pre-treatment by Oryeongsan	Post-treatment by Oryeongsan
Sample size	54	54	50	50
Age (years)	56.4 (51.2–64.5)	57.0(51.8–65.1)	57.2 (52.4–69.1)	57.8 (53.0–69.7)
Men (%)	48	48	52	48
BMI (kg/m ²)	24.8 (23.3–26.4)	24.7 (23.1–25.9)	24.5 (23.8–26.1)	24.3 (23.4–25.4)
Proteinuria (mg/24 h)	865.2 (624.3–957.4)	513.1 (389.3–756.4)**	895.4 (645.2–947.5)	578.5 (402.7–718.6) **
Urine ACR (mg/g)	527.4 (385.2–574.7)	314.8 (239.8–459.8) **	542.4 (397.5–574.9)	358.7 (249.6–445.8) **
eGFR (ml/min/1.73 m ²)	54.5 (42.5–75.8)	62.4 (52.1–78.9) **	55.8 (45.8–72.4)	65.7 (49.8–75.5) **

* $P < 0.05$, ** $P < 0.01$ compared with pre-treatment patients.

3.8. Gene and protein expression of Nrf2 pathway

Compared with CKD patients with microalbuminuria, CKD patients with macroalbuminuria showed a significant up-regulation in Kelch-like ECH-associated protein 1 (Keap1) and nuclear translocation of Nrf2 mRNA expression, indicating activation of impaired Nrf2 pathway (Fig. 6A). Activation of Keap1/Nrf2 signaling was accompanied by a significant up-regulation of catalase and heme oxygenase-1 (HO-1) mRNA expression as well as down-regulation of glutamate cysteine ligase catalytic subunit (GCLC), NAD(P)H quinone oxidoreductase 1 (NQO1) and glutathione peroxidase (GPX) mRNA expression. However, GCLM mRNA expression was not significantly altered in CKD patients with macroalbuminuria. Moreover, CKD patients with macroalbuminuria showed a marked reduction in nuclear Nrf2 protein expression and a significant increase in Keap1 protein expression. In addition, the expression of Nrf2 target genes including catalase, HO-1, GCLC, glutamate-cysteine ligase modifier subunit (GCLM), NQO1 and GPX was also significantly decreased (Fig. 6B). These findings point to the significant impaired activation of the Nrf2 pathway in CKD patients.

3.9. Gene and protein expression of Wnt/ β -catenin pathway

Wnt/ β -catenin signaling pathway was closely associated with progressive CKD [33,41–45]. Compared with CKD patients with microalbuminuria, CKD patients with macroalbuminuria exhibited a significant up-regulation in Wnt1, Wnt4 and β -catenin mRNA expression, indicating activation of Wnt/ β -catenin pathway. Activation of Wnt/ β -catenin signaling was accompanied by significant up-regulation of its target genes including Twist, Snail1, PAI-1, MMP-7 and FSP1 (Fig. 7A).

Western blotting analysis showed that the protein expressions of Wnt1, cytoplasmic β -catenin, nuclear β -catenin and nuclear active β -catenin were dramatically up-regulated in CKD patients with macroalbuminuria compared with those with microalbuminuria. Except for Snail1, significant up-regulation of Twist, PAI-1 and MMP-7 protein expression were observed in CKD patients (Fig. 7B).

We also examined the expression and localization of Wnt/ β -catenin and its target proteins. As shown in Fig. 7C and Fig. 8A, the expression

of Wnt1, PAI-1 and MMP-7 proteins were predominantly induced in proximal tubular epithelium and glomerular from CKD patients. The expression of active β -catenin protein and Twist and Snail1 proteins were predominantly induced in nuclei of renal tubular epithelium in CKD patients. FSP1, derived from epithelial mesenchymal transition, was a marker of fibroblasts in different tissues undergoing tissue remodeling, and the expression of FSP1 protein was significantly increased in tubulo-interstitium of CKD patients. In addition, the alteration of Wnt/ β -catenin and its target proteins showed the stronger expression in CKD patients with macroalbuminuria than those with microalbuminuria (Fig. 8B). These results indicate that Wnt/ β -catenin pathway could be a novel therapeutic target for the intervention of CKD.

4. Discussion

Inflammation and CKD are both intimately implicated in cardiovascular diseases. Our previous studies revealed that lipid metabolism was evidently altered in CKD patients. Additionally, we also discovered that protein expressions of plasma inflammation and oxidative stress were closely associated with abnormal lipid metabolism in both patients and rats with CKD. Nevertheless, whether inflammatory biomarkers and abnormal lipid metabolites are involved in the different degrees of albuminuria and kidney dysfunction after accounting for traditional cardiovascular disease risk factors remains to be determined. In this study, we first uncovered the association of plasma inflammation, oxidative stress, Wnt/ β -catenin, albuminuria and lipid metabolism in patients with CKD stages 3 to 5. The association of inflammation with urinary albumin excretion had been widely reported in previous studies, and inflammatory biomarkers, such as C-reactive protein, tumor necrosis factor- α , intercellular adhesion molecule 1, MCP-1, interleukin-6, tumor necrosis factor receptor 2 and fibrinogen, were deeply implicated in albuminuria and kidney dysfunction [46–48]. In particular, serum cystatin C was an index of renal function and substantial variability in soluble tumor necrosis factor receptor 2 was attributable to CKD and cystatin C [49], which was consistent with activated I κ B/NF- κ B and Keap1/Nrf2 pathways in CKD patients with

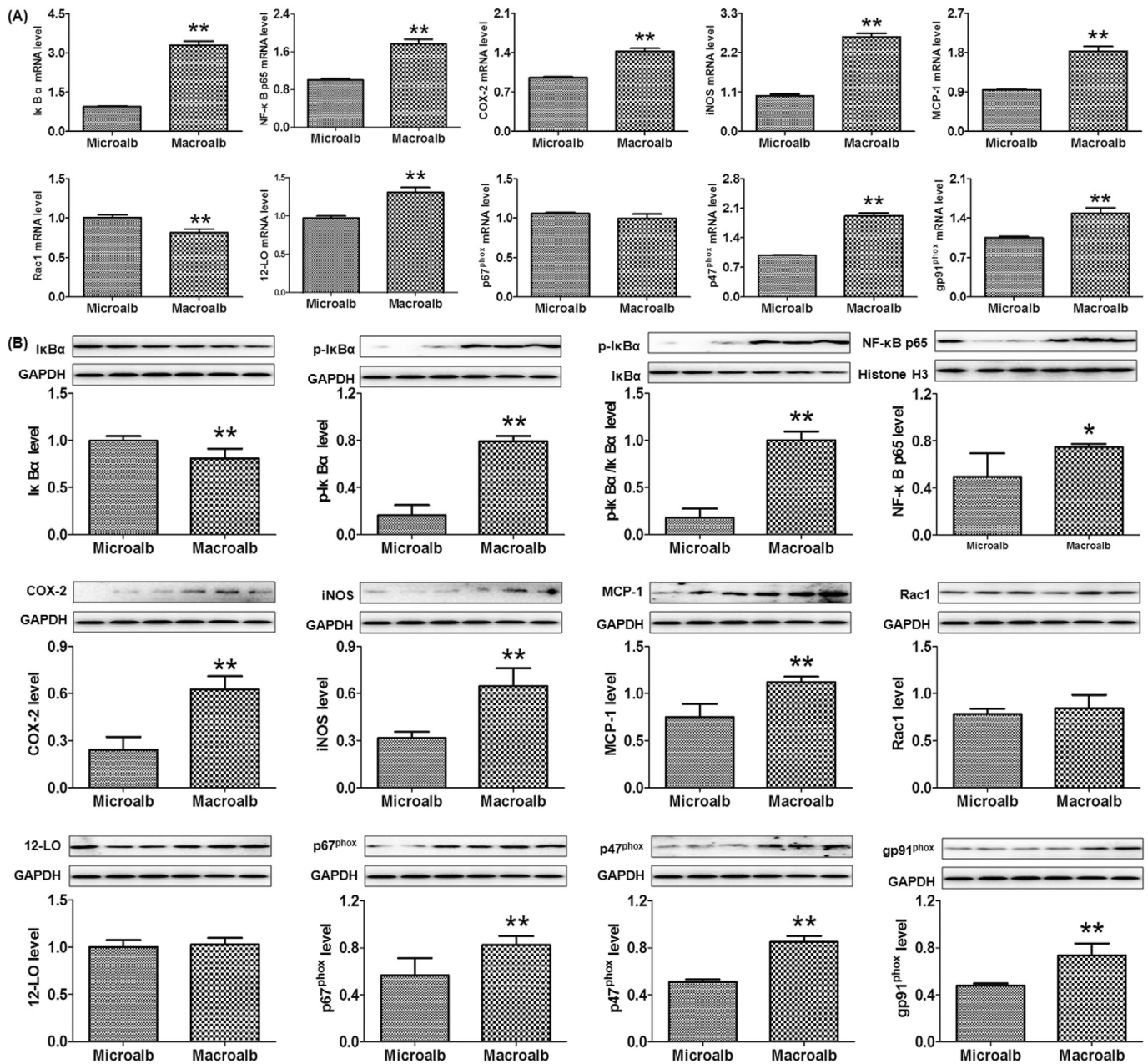


Fig. 5. Expression of NF- κ B and its target genes and proteins in CKD patients with microalbuminuria and macroalbuminuria. (A) qRT-PCR of the expression mRNA of NF- κ B p65 and its target genes including COX-2, iNOS, MCP-1, Rac1, 12-LO, p67^{phox}, P47^{phox} and gp91^{phox} in CKD patients with microalbuminuria and macroalbuminuria. (B) Representative Western blotting analyses and their quantitative analyses the expressions of p65 active subunit of NF- κ B protein and its target proteins including COX-2, iNOS, MCP-1, Rac1, 12-LO, p67^{phox}, P47^{phox} and gp91^{phox} in the plasma of CKD patients with microalbuminuria and macroalbuminuria. * $P < 0.05$, ** $P < 0.01$ compared with the CKD patients with microalbuminuria.

microalbuminuria and macroalbuminuria. Furthermore, sphingomyelin was a significant regressor of albuminuria [15]. Other metabolomics also demonstrated that 19 metabolites distinguished diabetic nephropathy with macroalbuminuria from those without albuminuria [50], and these metabolites were significantly correlated with urinary ACR, indicating lipid metabolism is inseparably associated with the development of CKD patients with albuminuria. Apart from above-mentioned factors, inflammation was involved in the Wnt/ β -catenin pathway of renal fibrosis [14]. Taken together, NF- κ B/Nrf2 and Wnt/ β -catenin pathways as well as significantly altered lipid metabolism contributed to the aggravation of albuminuria in CKD patients.

Four lipid species that showed great potential in the discrimination of CKD patients with microalbuminuria and healthy controls were selected by logistic regression analysis. In addition, six lipid species that

played pivotal roles in the discrimination of CKD patients with microalbuminuria and macroalbuminuria were selected by logistic LASSO regression. Our study showed that five fatty acids were contained in ten biomarkers the results indicated fatty acid metabolism was closely associated with albuminuria change. Further analysis found that polyunsaturated fatty acids (PUFA) including DHA, DTA and TTA were dramatically decreased and saturated fatty acids (SFA), such as 5,8-TDA and EDA were obviously increased in CKD patients with microalbuminuria and macroalbuminuria. This was consistent with the earlier studies that plasma free fatty acids and SFA were significantly elevated in the pre-hemodialysis samples of ESRD patients compared with healthy controls [51]. We also identified DTA and DHA in the adenine-induced rats with CKD in our previous studies [52,53]. In fact, plasma SFA was associated with the incidence of sudden cardiac death

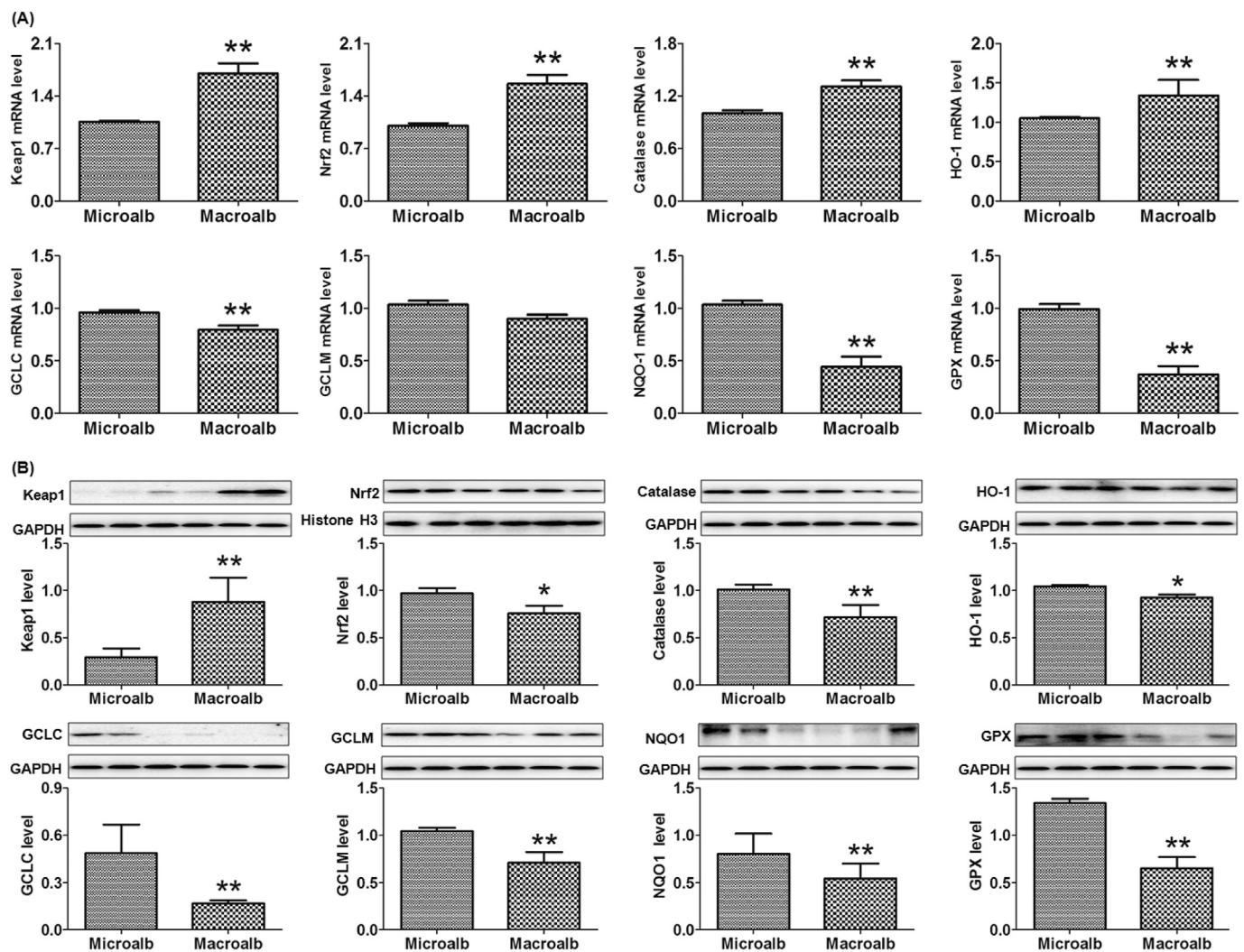


Fig. 6. Expression of Nrf2 and its target genes and proteins in CKD patients with microalbuminuria and macroalbuminuria. (A) qRT-PCR analysis of Nrf2 mRNA and its target genes including catalase, HO-1, GCLC, GCLM, NQO1 and GPX mRNA, in the CKD patients with microalbuminuria and macroalbuminuria. (B) Representative Western blotting analyses and their quantitative analyses of Nrf2 protein and its target proteins including catalase, HO-1, GCLC, GCLM, NQO1 and GPX in the CKD patients with microalbuminuria and macroalbuminuria. *P < 0.05, **P < 0.01 compared with the CKD patients with microalbuminuria.

in patients with hemodialysis [54], which was largely due to the impairment of fatty acid oxidation (FAO) in the tubular epithelial cells of CKD patients and animal models with interstitial fibrosis [55]. The abnormal FAO contributed to the impairment of mitochondrial adenosine triphosphate generation and enhancement of reactive oxygen species (ROS) production, leading to the occurrence of tubular epithelial cell death, inflammation, oxidative stress and interstitial fibrosis.

Normally, the uptake, oxidation and synthesis of fatty acids are tightly balanced to avoid intracellular lipid accumulation. The uptake of long-chain fatty acids is facilitated by long-chain fatty acid transporter CD36 [56], while carnitine palmitoyltransferase 1 is of paramount importance to the metabolism of fatty acids by combining with carnitine and transporting into the mitochondria, which serves as the rate-limiting enzyme of fatty acid oxidation [57]. FAO occurs in the mitochondria, the impairment of which leads to mitochondrial dysfunction and defective oxidative phosphorylation. In addition, mitochondrial dysfunction plays pivotal roles in the pathogenesis of CKD [58]. PUFA are very susceptible to ROS-mediated peroxidation, which makes them attractive targets of endocytosis by macrophages. Mounting studies revealed that PUFA deficiency was implicated in the progression in CKD, and long-chain PUFA supplement could mitigate inflammatory and oxidative stress via lowering production of inflammatory eicosanoids and cytokines, adhesion molecules and ROS

[59]. Therefore, PUFA deficiency contributed to inflammation and oxidative stress in CKD [60,61]. Therefore, the changes of fatty acids can contribute to the inflammation and oxidative stress.

Gangliosides are glycosphingolipids or oligoglycosylceramides with one or more sialic acids linked on the sugar chain. Ganglioside is a component of cell membrane that plays a critical role in the modulation of signal transduction [62,63]. Gangliosides amount to approximately 6% of the weight of lipids in brain, but gangliosides are found in all animal tissues [64]. A lot of gangliosides were firstly identified from the serum of CKD patients with albuminuria in our study, among which ganglioside GD3 (d18:1/26:0) and ganglioside GD2 (d18:1/18:0) were used to distinguish CKD patients with microalbuminuria from healthy controls as well as CKD patients with microalbuminuria and macroalbuminuria, respectively. Immunohistochemical analyses indicated that ganglioside GM3 was distributed in renal proximal tubules and glomeruli. Immunoelectron microscopy showed that ganglioside GM3 was localized in Golgi region of renal proximal tubule cells and the foot process of podocyte [65]. Ganglioside GM3 might take a part of the negative electric charge on the podocyte surface and multiple bioactivities of ganglioside GM3 played important roles for maintaining glomerular physiological function. Increased gangliosides in renal cell carcinoma contributed to the immune suppression observed in cancer patients. Ganglioside-induced T-cell killing was related to the caspase-

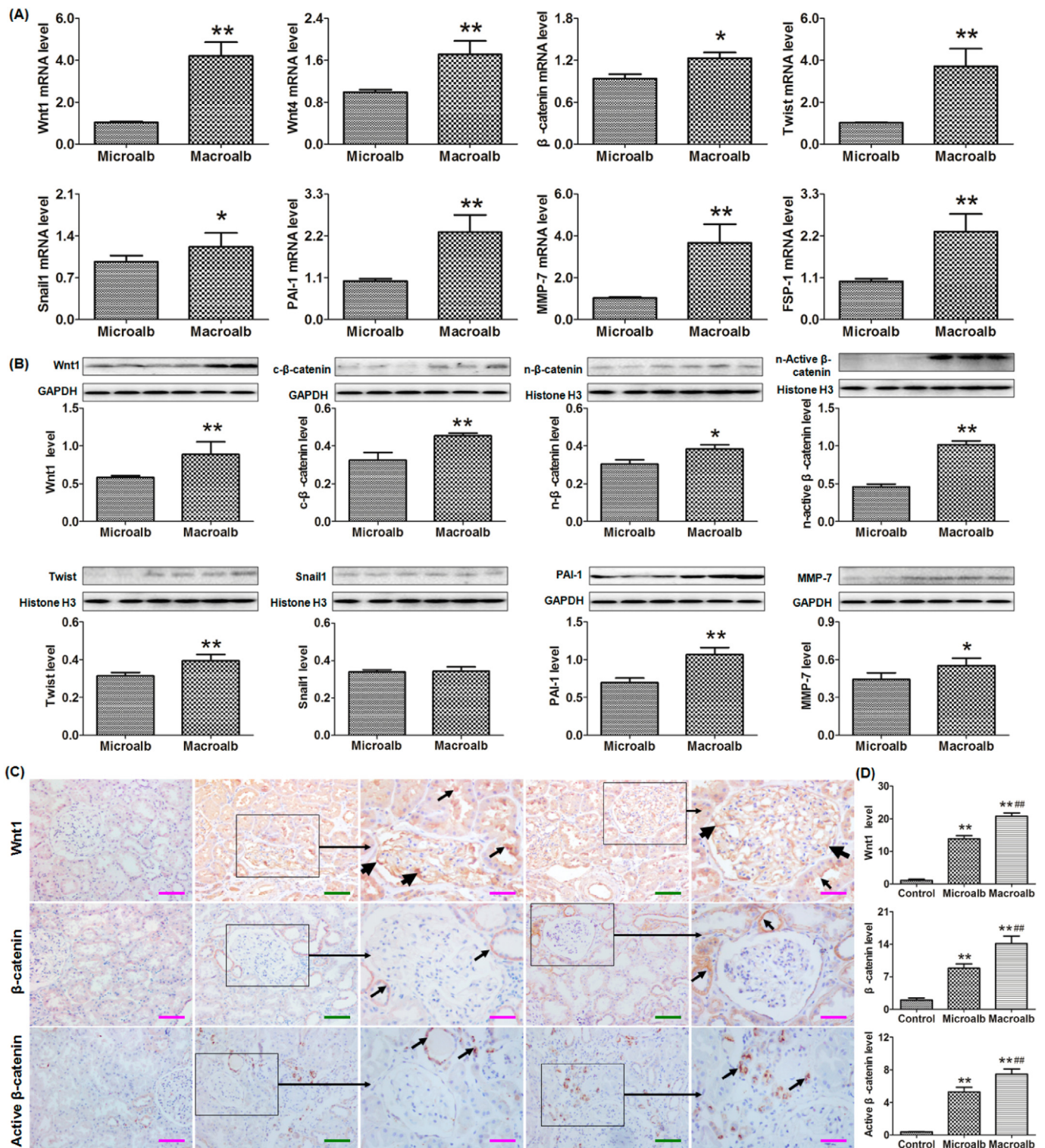


Fig. 7. Expression of β -catenin and its target genes and proteins in CKD patients with microalbuminuria and macroalbuminuria. (A) qRT-PCR of Wnt1, Wnt4 and β -catenin as well as its target genes, including Twist, Snail1, PAI-1, MMP-7 and FSP1, in the CKD patients with microalbuminuria and macroalbuminuria. (B) Representative Western blotting analyses and their quantitative analyses of Wnt1, cytoplasmic β -catenin, nuclear β -catenin as well as nuclear active β -catenin and its target proteins, including Twist, Snail1, PAI-1 and MMP-7, in the CKD patients with microalbuminuria and macroalbuminuria. * $P < 0.05$, ** $P < 0.01$ compared with the CKD patients with microalbuminuria. (C) Immunohistochemical staining and (D) semi-quantitative analyses of Wnt/ β -catenin signaling pathway in CKD patients with microalbuminuria and macroalbuminuria. Paraffin kidney sections were used for immunohistochemical staining of Wnt1, β -catenin and active β -catenin in the kidney of healthy controls, CKD patients with microalbuminuria and macroalbuminuria. Immunohistochemical staining showed a strong expression of Wnt1 in proximal tubular epithelium (thin arrow) and glomerular (thick arrow) of kidney tissue from the CKD patients with microalbuminuria and macroalbuminuria. The β -catenin only showed a strong expression in proximal tubular epithelium (thin arrow) of kidney tissue from the CKD patients with microalbuminuria and macroalbuminuria. The active β -catenin only showed a strong expression in nuclei of proximal tubular epithelium (thin arrow) of kidney tissue from the CKD patients with microalbuminuria and macroalbuminuria. * $P < 0.05$, ** $P < 0.01$ compared with healthy controls; ### $P < 0.01$ compared with CKD patients with microalbuminuria. Pink bar = 20 μ m; green bar = 35 μ m.

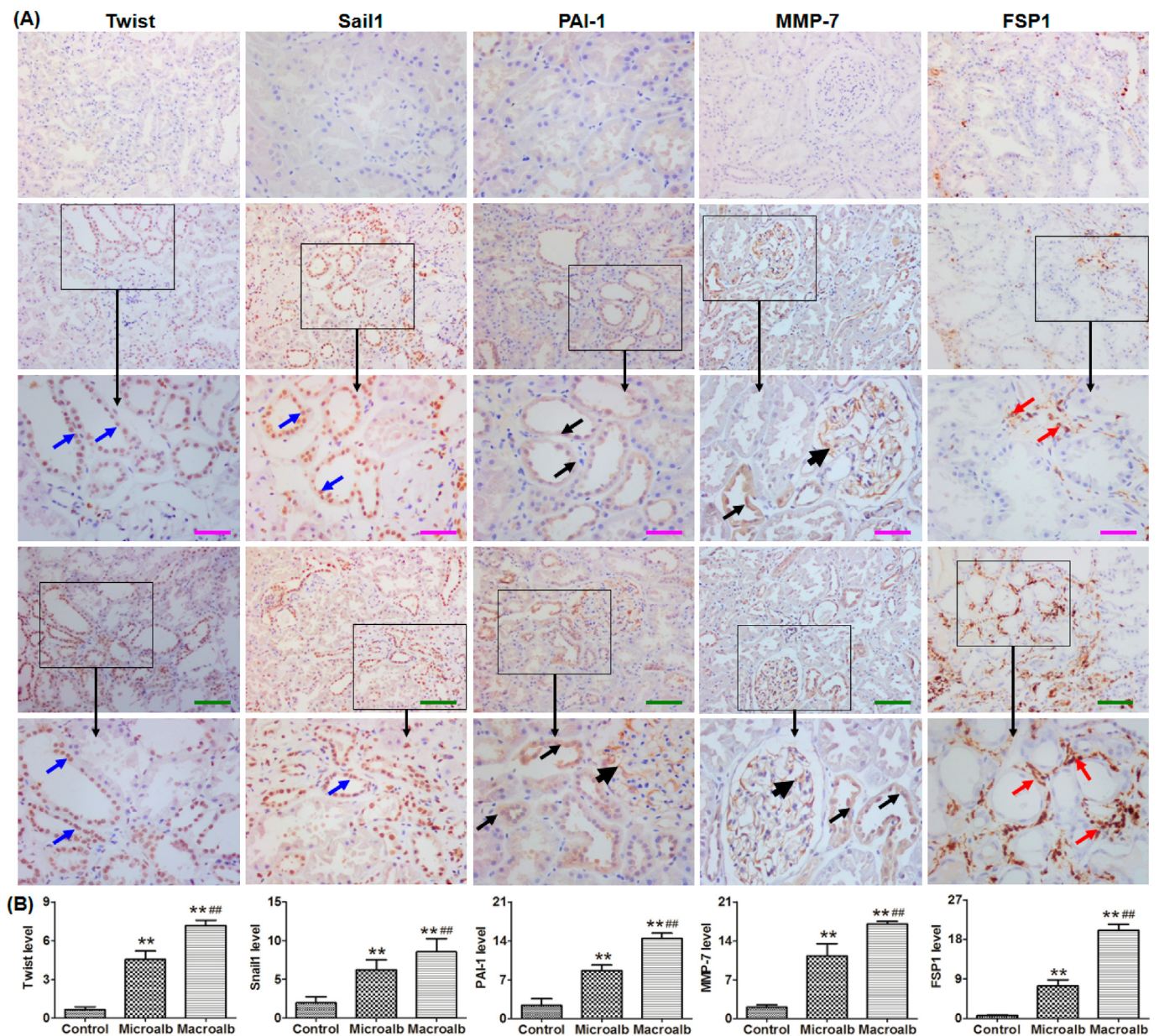


Fig. 8. The expression of target genes of Wnt/ β -catenin pathway in CKD patients with microalbuminuria and macroalbuminuria. (A) Immunohistochemical findings of Twist, Snail1, PAI-1, MMP-7 and FSP1 antibody in the kidney of healthy controls, CKD patients with microalbuminuria and macroalbuminuria. Paraffin kidney sections were used for immunohistochemical staining for Twist, Snail1, PAI-1, MMP-7 and FSP1. Immunohistochemical staining showed an expression of nuclear Twist and Snail1 in proximal tubular epithelial cells (blue arrow) of kidney tissue from the CKD patients with microalbuminuria and macroalbuminuria. An expression of PAI-1 and MMP-7 in proximal tubular epithelium (thin arrow) and glomerular (thick arrow) of kidney tissue from the CKD patients with microalbuminuria and macroalbuminuria. Immunohistochemical staining also showed an expression of FSP1 in renal tubulo-interstitium (red arrow) of kidney tissue from the CKD patients with microalbuminuria and macroalbuminuria. (B) Quantitative analyses of target genes of Wnt/ β -catenin in CKD patients with microalbuminuria and macroalbuminuria. * $P < 0.05$, ** $P < 0.01$ compared with healthy controls; *** $P < 0.01$ compared with CKD patients with microalbuminuria. Pink bar = 20 μ m; green bar = 35 μ m.

dependent degradation of NF- κ B-inducible and anti-apoptotic proteins [66]. It was reported that ROS were significantly increased in GM2⁺ but not GM2⁻ T cells from patients with renal cell carcinoma. Immunocytometric analysis showed that significantly increased ganglioside GD2 and ganglioside GD3 rather than ganglioside GD1a were observed in T cells of patients with increased apoptosis in the GD2⁺ and GD3⁺ cells. Moreover, increasing evidence suggested that ganglioside might play a prominent role in CKD patients with albuminuria. Therefore, gangliosides might be exploited for novel therapeutic targets for CKD patients.

In conclusion, abnormal lipid metabolism was intimately associated with PPAR γ , TRP channels and RAS signaling, which were deeply

involved in the activation of I κ B/NF- κ B and Keap1/Nrf2 pathways. Gangliosides were first identified and might be promising therapeutic targets for CKD patients with the different degree of albuminuria. Of note, this is the first time that the association of plasma inflammation, oxidative stress, Wnt/ β -catenin and lipid metabolism has been revealed in CKD patients with microalbuminuria and macroalbuminuria.

Transparency document

The [Transparency document](#) associated with this article can be found, in online version.

Declaration of Competing Interest

The authors have nothing to disclose.

Acknowledgements

This study was supported by the Shaanxi Science and Technology Plan Project (2019ZDLSF04-04-02) and National Natural Science Foundation of China (81673578, 81603271).

Duality of interest

We declare no competing interests.

Contribution statement

Y.Y.Z. and Y.G. conceived and designed the project, and managed the study. S.X.M., Y.Q.S., W.S., J.R.M., X.Y.Y., and L.Z. made clinical diagnosis, recruited subjects and performed intervention. S.X.M., Y.Q.S., W.S., J.R.M. and X.Y.Y. collected samples and clinical phenotypes. Y.L.F., Y.G. and Y.Y.Z. performed bioinformatics analyses. Y.L.F., Y.Y.Z., and H.C. performed metabolomics profiling and data analysis. Y.Y.Z., Y.G., D.Q.C. and N.D.V. wrote the manuscript. N.D.V. contributed to text revision.

Appendix A. Supplementary data

Supplementary data to this article can be found online at <https://doi.org/10.1016/j.bbadis.2019.05.010>.

References

- [1] A.C. Webster, E.V. Nagler, R.L. Morton, P. Masson, Chronic kidney disease, *Lancet* 389 (2017) 1238–1252.
- [2] D.Q. Chen, G. Cao, H. Chen, C.P. Argyropoulos, H. Yu, W. Su, L. Chen, D.C. Samuels, S. Zhuang, G.P. Bayliss, S. Zhao, X.Y. Yu, N.D. Vaziri, M. Wang, D. Liu, J.R. Mao, S.X. Ma, J. Zhao, Y. Zhang, Y.Q. Shang, H. Kang, F. Ye, X.H. Cheng, X.R. Li, L. Zhang, M.X. Meng, Y. Guo, Y.Y. Zhao, Identification of serum metabolites associating with chronic kidney disease progression and anti-fibrotic effect of 5-methoxytryptophan, *Nat. Commun.* 10 (2019) 1476.
- [3] C.P. Kovessy, E.H. Lott, J.L. Lu, S.M. Malakauskas, J.Z. Ma, M.Z. Molnar, K. Kalantar-Zadeh, Outcomes associated with microalbuminuria: effect modification by chronic kidney disease, *J. Am. Coll. Cardiol.* 61 (2013) 1626–1633.
- [4] N.D. Vaziri, Disorders of lipid metabolism in nephrotic syndrome: mechanisms and consequences, *Kidney Int.* 90 (2016) 41–52.
- [5] M.R. Hager, A.D. Narla, L.R. Tannock, Dyslipidemia in patients with chronic kidney disease, *Rev. Endocr. Metab. Disord.* 18 (2017) 29–40.
- [6] R.J. Martens, J.P. Kooman, C.D. Stehouwer, P.C. Dagnelie, C.J. van der Kallen, A. Koster, A.A. Kroon, K.M. Leunissen, G. Nijpels, F.M. van der Sande, N.C. Schaper, S.J. Sep, M.P. van Bortel, M.T. Schram, R.M. Henry, Estimated GFR, albuminuria, and cognitive performance: the Maastricht study, *Am. J. Kidney Dis.* 69 (2017) 179–191.
- [7] Y.Y. Zhao, X.L. Cheng, F. Wei, X. Bai, X.J. Tan, R.C. Lin, Q. Mei, Intrarenal metabolomic investigation of chronic kidney disease and its TGF- β 1 mechanism in induced-adenine rats using UPLC Q-TOF/HSMS/MS^E, *J. Proteome Res.* 12 (2013) 2692–2703.
- [8] Z.H. Zhang, H. Chen, N.D. Vaziri, J.R. Mao, L. Zhang, X. Bai, Y.Y. Zhao, Metabolomic signatures of chronic kidney disease of diverse etiologies in the rats and humans, *J. Proteome Res.* 15 (2016) 3802–3812.
- [9] N.D. Vaziri, HDL abnormalities in nephrotic syndrome and chronic kidney disease, *Nat. Rev. Nephrol.* 12 (2016) 37–47.
- [10] H. Chen, L. Chen, D. Liu, D.Q. Chen, N.D. Vaziri, X.Y. Yu, L. Zhang, W. Su, X. Bai, Y.Y. Zhao, Combined clinical phenotype and lipidomic analysis reveals the impact of chronic kidney disease on lipid metabolism, *J. Proteome Res.* 16 (2017) 1566–1578.
- [11] D.Q. Chen, Y.L. Feng, L. Chen, J.R. Liu, M. Wang, N.D. Vaziri, Y.Y. Zhao, Poricoic acid A enhances melatonin inhibition of AKI-to-CKD transition by regulating Gas6/Axl-NF- κ B/Nrf2 axis, *Free Radic. Biol. Med.* 134 (2019) 484–497.
- [12] Y.Y. Zhao, H.L. Wang, X.L. Cheng, F. Wei, X. Bai, R.C. Lin, N.D. Vaziri, Metabolomics analysis reveals the association between lipid abnormalities and oxidative stress, inflammation, fibrosis, and Nrf2 dysfunction in aristolochic acid-induced nephropathy, *Sci. Rep.* 5 (2015) 12936.
- [13] M.J. Pena, J. Jankowski, G. Heinze, M. Kohl, A. Heinzel, S.J. Bakker, R.T. Gansevoort, P. Rossing, D. de Zeeuw, H.J. Heerspink, V. Jankowski, Plasma proteomics classifiers improve risk prediction for renal disease in patients with hypertension or type 2 diabetes, *J. Hypertens.* 33 (2015) 2123–2132.
- [14] M. Edeling, G. Ragi, S. Huang, H. Pavenstadt, K. Susztak, Developmental signalling pathways in renal fibrosis: the roles of Notch, Wnt and Hedgehog, *Nat. Rev. Nephrol.* 12 (2016) 426–439.
- [15] V.P. Makinen, T. Tynkkynen, P. Soininen, C. Forsblom, T. Peltola, A.J. Kangas, P.H. Groop, M. Ala-Korpela, Sphingomyelin is associated with kidney disease in type 1 diabetes (The FinnDiane Study), *Metabolomics* 8 (2012) 369–375.
- [16] Y.Y. Zhao, X.L. Cheng, R.C. Lin, F. Wei, Lipidomics applications for disease biomarker discovery in mammal models, *Biomark. Med.* 9 (2015) 153–168.
- [17] Y.Y. Zhao, X.L. Cheng, R.C. Lin, Lipidomics applications for discovering biomarkers of diseases in clinical chemistry, *Int. Rev. Cell Mol. Biol.* 313 (2014) 1–26.
- [18] Y.Y. Zhao, H. Miao, X.L. Cheng, F. Wei, Lipidomics: novel insight into the biochemical mechanism of lipid metabolism and dysregulation-associated disease, *Chem. Biol. Interact.* 240 (2015) 220–238.
- [19] H. Chen, H. Miao, Y.L. Feng, Y.Y. Zhao, R.C. Lin, Metabolomics in dyslipidemia, *Adv. Clin. Chem.* 66 (2014) 101–119.
- [20] Y.Y. Zhao, N.D. Vaziri, R.C. Lin, Lipidomics: new insight into kidney disease, *Adv. Clin. Chem.* 68 (2015) 153–175.
- [21] Y.Y. Zhao, Metabolomics in chronic kidney disease, *Clin. Chim. Acta* 422 (2013) 59–69.
- [22] Y.Y. Zhao, R.C. Lin, Metabolomics in nephrotoxicity, *Adv. Clin. Chem.* 65 (2014) 69–89.
- [23] S. Li, P. Xu, L. Han, W. Mao, Y. Wang, G. Luo, N. Yang, Disease-syndrome combination modeling: metabolomic strategy for the pathogenesis of chronic kidney disease, *Sci. Rep.* 7 (2017) 8830.
- [24] Y.Y. Zhao, X.L. Cheng, J.H. Cui, X.R. Yan, F. Wei, X. Bai, R.C. Lin, Effect of ergosta-4,6,8(14),22-tetraen-3-one (ergone) on adenine-induced chronic renal failure rat: a serum metabolomic study based on ultra performance liquid chromatography/high-sensitivity mass spectrometry coupled with MassLynx i-FIT algorithm, *Clin. Chim. Acta* 413 (2012) 1438–1445.
- [25] Y.Y. Zhao, S.P. Wu, S. Liu, Y. Zhang, R.C. Lin, Ultra-performance liquid chromatography-mass spectrometry as a sensitive and powerful technology in lipidomic applications, *Chem. Biol. Interact.* 220 (2014) 181–192.
- [26] H. Miao, H. Chen, S. Pei, X. Bai, N.D. Vaziri, Y.Y. Zhao, Plasma lipidomics reveal profound perturbation of glycerophospholipids, fatty acids, and sphingolipids in diet-induced hyperlipidemia, *Chem. Biol. Interact.* 228 (2015) 79–87.
- [27] F. Dou, H. Miao, J.W. Wang, L. Chen, M. Wang, H. Chen, A.D. Wen, Y.Y. Zhao, An integrated lipidomics and phenotype study reveals protective effect and biochemical mechanism of traditionally used *Alisma orientale* Juzepzuk in chronic renal disease, *Front. Pharmacol.* 9 (2018) 53.
- [28] Z.H. Zhang, N.D. Vaziri, F. Wei, X.L. Cheng, X. Bai, Y.Y. Zhao, An integrated lipidomics and metabolomics reveal nephroprotective effect and biochemical mechanism of *Rheum officinale* in chronic renal failure, *Sci. Rep.* 6 (2016) 22151.
- [29] Y.Y. Zhao, J. Liu, X.L. Cheng, X. Bai, R.C. Lin, Urinary metabolomics study on biochemical changes in an experimental model of chronic renal failure by adenine based on UPLC Q-TOF/MS, *Clin. Chim. Acta* 413 (2012) 642–649.
- [30] H. Miao, Y.H. Zhao, N.D. Vaziri, D.D. Tang, H. Chen, H. Chen, M. Khazaeli, M. Tarbiat-Boldaji, L. Hataami, Y.Y. Zhao, Lipidomics biomarkers of diet-induced hyperlipidemia and its treatment with *Poria cocos*, *J. Agric. Food Chem.* 64 (2016) 969–979.
- [31] Z.H. Zhang, J.R. Mao, H. Chen, W. Su, Y. Zhang, L. Zhang, D.Q. Chen, Y.Y. Zhao, N.D. Vaziri, Removal of uremic retention products by hemodialysis is coupled with indiscriminate loss of vital metabolites, *Clin. Biochem.* 50 (2017) 1078–1086.
- [32] N.K. Foundation, K/DOQI clinical practice guidelines for chronic kidney disease: evaluation, classification, and stratification, *Am. J. Kidney Dis.* 39 (2002) S1–266.
- [33] D.Q. Chen, G. Cao, H. Chen, D. Liu, W. Su, X.Y. Yu, N.D. Vaziri, X.H. Liu, X. Bai, L. Zhang, Y.Y. Zhao, Gene and protein expressions and metabolomics exhibit activated redox signaling and Wnt/ β -catenin pathway are associated with metabolite dysfunction in patients with chronic kidney disease, *Redox Biol.* 12 (2017) 505–521.
- [34] H. Chen, G. Cao, D.Q. Chen, M. Wang, N.D. Vaziri, Z.H. Zhang, J.R. Mao, X. Bai, Y.Y. Zhao, Metabolomics insights into activated redox signaling and lipid metabolism dysfunction in chronic kidney disease progression, *Redox Biol.* 10 (2016) 168–178.
- [35] L. Chen, G. Cao, M. Wang, Y.L. Feng, D.Q. Chen, N.D. Vaziri, S. Zhuang, Y.Y. Zhao, The matrix metalloproteinase-13 inhibitor poricoic acid ZI ameliorates renal fibrosis by mitigating epithelial-mesenchymal transition, *Mol. Nutr. Food Res.* 63 (2019) e1900132.
- [36] M. Wang, D.Q. Chen, L. Chen, G. Cao, H. Zhao, D. Liu, N.D. Vaziri, Y. Guo, Y.Y. Zhao, Novel inhibitors of the cellular renin-angiotensin system components, poricoic acids, target Smad3 phosphorylation and Wnt/ β -catenin pathway against renal fibrosis, *Br. J. Pharmacol.* 175 (2018) 2689–2708.
- [37] M. Wang, D.Q. Chen, M.C. Wang, H. Chen, L. Chen, D. Liu, H. Zhao, Y.Y. Zhao, Poricoic acid ZA, a novel RAS inhibitor, attenuates tubulo-interstitial fibrosis and podocyte injury by inhibiting TGF- β /Smad signaling pathway, *Phytomedicine* 36 (2017) 243–253.
- [38] Z.H. Zhang, F. Wei, N.D. Vaziri, X.L. Cheng, X. Bai, R.C. Lin, Y.Y. Zhao, Metabolomics insights into chronic kidney disease and modulatory effect of rhubarb against tubulointerstitial fibrosis, *Sci. Rep.* 5 (2015) 14472.
- [39] P. Qin, X. Tang, M.M. Elloso, D.C. Harnish, Bile acids induce adhesion molecule expression in endothelial cells through activation of reactive oxygen species, NF- κ B, and p38, *Am. J. Physiol. Heart Circ. Physiol.* 291 (2006) H741–H747.
- [40] E. Halilbasic, C. Fuchs, S. Traussnigg, M. Trauner, Farnesoid X Receptor agonists and other bile acid signaling strategies for treatment of liver disease, *Dig. Dis.* 34 (2016) 580–588.
- [41] D.Q. Chen, Y.L. Feng, G. Cao, Y.Y. Zhao, Natural products as a source for anti-fibrosis therapy, *Trends Pharmacol. Sci.* 39 (2018) 937–952.

- [42] D.Q. Chen, H.H. Hu, Y.N. Wang, Y.L. Feng, G. Cao, Y.Y. Zhao, Natural products for the prevention and treatment of kidney disease, *Phytomedicine* 50 (2018) 50–60.
- [43] L. Chen, D.Q. Chen, M. Wang, D. Liu, H. Chen, F. Dou, N.D. Vaziri, Y.Y. Zhao, Role of RAS/Wnt/ β -catenin axis activation in the pathogenesis of podocyte injury and tubulo-interstitial nephropathy, *Chem. Biol. Interact.* 273 (2017) 56–72.
- [44] M. Wang, D.Q. Chen, L. Chen, H. Zhao, D. Liu, Z.H. Zhang, N.D. Vaziri, Y. Guo, Y.Y. Zhao, G. Cao, Novel RAS inhibitors poricoic acid ZG and poricoic acid ZH attenuate renal fibrosis via Wnt/ β -catenin pathway and targeted phosphorylation of smad3 signaling, *J. Agric. Food Chem.* 66 (2018) 1828–1842.
- [45] H. Chen, T. Yang, M.C. Wang, D.Q. Chen, Y. Yang, Y.Y. Zhao, Novel RAS inhibitor 25-O-methylalisol F attenuates epithelial-to-mesenchymal transition and tubulo-interstitial fibrosis by selectively inhibiting TGF- β -mediated Smad3 phosphorylation, *Phytomedicine* 42 (2018) 207–218.
- [46] A.E. DeClevles, K. Sharma, Novel targets of antifibrotic and anti-inflammatory treatment in CKD, *Nat. Rev. Nephrol.* 10 (2014) 257–267.
- [47] H.M. Kok, L.L. Falke, R. Goldschmeding, T.Q. Nguyen, Targeting CTGF, EGF and PDGF pathways to prevent progression of kidney disease, *Nat. Rev. Nephrol.* 10 (2014) 700–711.
- [48] O.J. Wouters, D.J. O'Donoghue, J. Ritchie, P.G. Kanavos, A.S. Narva, Early chronic kidney disease: diagnosis, management and models of care, *Nat. Rev. Nephrol.* 11 (2015) 491–502.
- [49] A. Upadhyay, M.G. Larson, C.Y. Guo, R.S. Vasani, I. Lipinska, C.J. O'Donnell, S. Kathiresan, J.B. Meigs, J.F. Keaney Jr., J. Rong, E.J. Benjamin, C.S. Fox, Inflammation, kidney function and albuminuria in the Framingham offspring cohort, *Nephrol. Dial. Transplant.* 26 (2011) 920–926.
- [50] A. Hirayama, E. Nakashima, M. Sugimoto, S. Akiyama, W. Sato, S. Maruyama, S. Matsuo, M. Tomita, Y. Yuzawa, T. Soga, Metabolic profiling reveals new serum biomarkers for differentiating diabetic nephropathy, *Anal. Bioanal. Chem.* 404 (2012) 3101–3109.
- [51] L. Wang, C. Hu, S. Liu, M. Chang, P. Gao, L. Wang, Z. Pan, G. Xu, Plasma lipidomics investigation of hemodialysis effects by using liquid chromatography-mass spectrometry, *J. Proteome Res.* 15 (2016) 1986–1994.
- [52] D.Q. Chen, H. Chen, L. Chen, N.D. Vaziri, M. Wang, X.R. Li, Y.Y. Zhao, The link between phenotype and fatty acid metabolism in advanced chronic kidney disease, *Nephrol. Dial. Transplant.* 32 (2017) 1154–1166.
- [53] Y.Y. Zhao, P. Lei, D.Q. Chen, Y.L. Feng, X. Bai, Renal metabolic profiling of early renal injury and renoprotective effects of *Poria cocos* epidermis using UPLC Q-TOF/HSMS/MS^E, *J. Pharm. Biomed. Anal.* 81–82 (2013) 202–209.
- [54] A.N. Friedman, Z. Yu, C. Denski, H. Tamez, J. Wenger, R. Thadhani, Y. Li, B. Watkins, Fatty acids and other risk factors for sudden cardiac death in patients starting hemodialysis, *Am. J. Nephrol.* 38 (2013) 12–18.
- [55] H.M. Kang, S.H. Ahn, P. Choi, Y.A. Ko, S.H. Han, F. Chinga, A.S. Park, J. Tao, K. Sharma, J. Pullman, E.P. Bottinger, I.J. Goldberg, K. Susztak, Defective fatty acid oxidation in renal tubular epithelial cells has a key role in kidney fibrosis development, *Nat. Med.* 21 (2015) 37–46.
- [56] K. Susztak, E. Ciccone, P. McCue, K. Sharma, E.P. Bottinger, Multiple metabolic hits converge on CD36 as novel mediator of tubular epithelial apoptosis in diabetic nephropathy, *PLoS Med.* 2 (2005) e45.
- [57] T.T. Schug, X. Li, Sirtuin 1 in lipid metabolism and obesity, *Ann. Med.* 43 (2011) 198–211.
- [58] L.L. Dugan, Y.H. You, S.S. Ali, M. Diamond-Stanic, S. Miyamoto, A.E. DeClevles, A. Andreyev, T. Quach, S. Ly, G. Shekhtman, W. Nguyen, A. Chepetan, T.P. Le, L. Wang, M. Xu, K.P. Paik, A. Fogo, B. Viollet, A. Murphy, F. Brosius, R.K. Naviaux, K. Sharma, AMPK dysregulation promotes diabetes-related reduction of superoxide and mitochondrial function, *J. Clin. Invest.* 123 (2013) 4888–4899.
- [59] P.C. Calder, N-3 polyunsaturated fatty acids, inflammation, and inflammatory diseases, *Am. J. Clin. Nutr.* 83 (2006) 1505s–1519s.
- [60] A.B. Irish, A.K. Viecelli, C.M. Hawley, L.S. Hooi, E.M. Pascoe, P.A. Paul-Brent, S.V. Badve, T.A. Mori, A. Cass, P.G. Kerr, D. Voss, L.M. Ong, K.R. Polkinghorne, Effect of fish oil supplementation and aspirin use on arteriovenous fistula failure in patients requiring hemodialysis: a randomized clinical trial, *JAMA Intern. Med.* 177 (2017) 184–193.
- [61] M. Svensson, J.J. Carrero, N-3 polyunsaturated fatty acids for the management of patients with chronic kidney disease, *J. Ren. Nutr.* 27 (2017) 147–150.
- [62] R.W. Ledeen, G. Wu, The multi-tasked life of GM1 ganglioside, a true factotum of nature, *Trends Biochem. Sci.* 40 (2015) 407–418.
- [63] S. Zhang, R.P. Bernthsson, W.H. Tepp, L. Tao, E.A. Johnson, P. Stenmark, M. Dong, Structural basis for the unique ganglioside and cell membrane recognition mechanism of botulinum neurotoxin DC, *Nat. Commun.* 8 (2017) 1637.
- [64] E. Sterner, M.L. Peach, M.C. Nicklaus, J.C. Gildersleeve, Therapeutic antibodies to ganglioside GD2 evolved from highly selective germline antibodies, *Cell Rep.* 20 (2017) 1681–1691.
- [65] T. Kaneko, Y. Tsubakihara, H. Fushimi, S. Yamaguchi, Y. Takabatake, H. Rakugi, H. Kawakami, Y. Isaka, Histochemical and immunoelectron microscopic analysis of ganglioside GM3 in human kidney, *Clin. Exp. Nephrol.* 19 (2015) 403–410.
- [66] G. Sa, T. Das, C. Moon, C.M. Hilston, P.A. Rayman, B.I. Rini, C.S. Tannenbaum, J.H. Finke, GD3, an overexpressed tumor-derived ganglioside, mediates the apoptosis of activated but not resting T cells, *Cancer Res.* 69 (2009) 3095–3104.